Accepted Manuscript

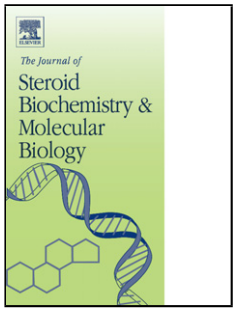

Title: Halogen-substituted anthranilic acid derivatives provide a novel chemical platform for androgen receptor antagonists

Authors: Daniela Roell, Thomas W. Rösler, Wiebke Hessenkemper, Florian Kraft, Monique Hauschild, Sophie Bartsch, Tsion E. Abraham, Adriaan B. Houtsmuller, Rudolf Matusch, Martin E. van Royen, Aria Baniahmad

PII: S0960-0760(18)30570-3
DOI: https://doi.org/10.1016/j.jsbmb.2018.12.005
Reference: SBMB 5269

To appear in: *Journal of Steroid Biochemistry & Molecular Biology*

Received date: 14 September 2018
Revised date: 4 December 2018
Accepted date: 7 December 2018

Please cite this article as: Roell D, Rösler TW, Hessenkemper W, Kraft F, Hauschild M, Bartsch S, Abraham TE, Houtsmuller AB, Matusch R, van Royen ME, Baniahmad A, Halogen-substituted anthranilic acid derivatives provide a novel chemical platform for androgen receptor antagonists, *Journal of Steroid Biochemistry and Molecular Biology* (2018), https://doi.org/10.1016/j.jsbmb.2018.12.005

Halogen-substituted anthranilic acid derivatives provide a novel chemical platform for androgen receptor antagonists

Daniela Roell[a,b,§], Thomas W. Rösler[c,§], Wiebke Hessenkemper[a], Florian Kraft[a], Monique Hauschild[a], Sophie Bartsch[a], Tsion E. Abraham[d], Adriaan B. Houtsmuller[d], Rudolf Matusch[c], Martin E. van Royen[d], Aria Baniahmad[a,*]

[a]Institute of Human Genetics, Jena University Hospital, Jena, Germany

[b]Integrated Research and Treatment Center, Center for Sepsis Control and Care (CSCC), Jena University Hospital, Jena, Germany

[c]Institute of Pharmaceutical Chemistry, Philipps-University, Marburg, Germany

[d]Department of Pathology and Erasmus Optical Imaging Center OIC, Erasmus MC, Rotterdam, The Netherlands

[§]These authors contributed equally.

*Corresponding author:

Jena University Hospital, Institute of Human Genetics, Am Klinikum 1, 07740 Jena, Germany

Ph.: +49-3641-9396820; Fax: +49-3641-99396822; aria.baniahmad@med.uni-jena.de

Graphical abstract

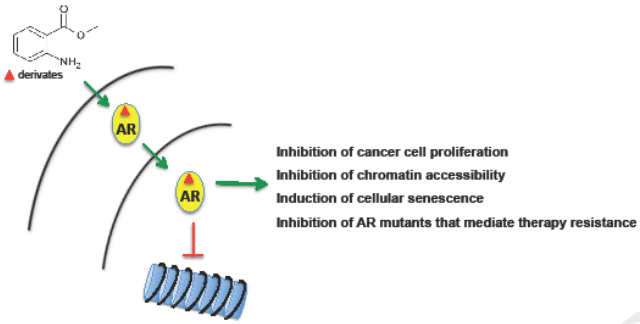

Highlights

- Identification of a novel chemical platform as a new lead structure that extends the diversity of known AR antagonists
- Novel AR antagonists possess a distinct mode of antagonizing AR-functions
- Novel AR antagonists inhibit prostate cancer cell proliferation
- Novel AR antagonists inhibit chromatin accessibility
- Novel AR antagonists induce cellular senescence
- Novel AR antagonists inhibit AR mutants that mediate therapy resistance

Abstract

Androgen receptor (AR) antagonists are used for hormone therapy of prostate cancer (PCa). However resistance to the treatment occur eventually. One possible reason is the occurrence of AR mutations that prevent inhibition of AR-mediated transactivation by antagonists. To offer in future more options to inhibit AR signaling, novel chemical lead structures for new AR antagonists would be beneficial. Here we analyzed structure-activity relationships of a battery of 36 non-steroidal structural variants of methyl anthranilate including 23 novel synthesized compounds. We identified structural requirements that lead to more potent AR antagonists. Specific compounds inhibit the transactivation of wild-type AR as well as AR mutants that render treatment resistance to hydroxyflutamide, bicalutamide and the second-generation AR antagonist enzalutamide. This suggests a distinct mode of inhibiting the AR compared to the clinically used compounds. Competition assays suggest binding of these compounds to the AR ligand binding domain and inhibit PCa cell proliferation. Moreover, active compounds induce cellular senescence despite inhibition of AR-mediated transactivation indicating a transactivation-independent AR-pathway. In line with this, fluorescence resonance after photobleaching (FRAP) - assays reveal higher mobility of the AR in the cell nuclei. Mechanistically, fluorescence resonance energy transfer (FRET) - assays indicate that the amino-carboxy (N/C)-interaction of the AR is not affected, which is in contrast to known AR-antagonists. This suggests a mechanistically novel mode of AR-antagonism. Together, these findings indicate the identification of a novel chemical platform as a new lead structure that extends the diversity of known AR antagonists and possesses a distinct mode of antagonizing AR-function.

Abbreviations: AR, androgen receptor; Cas, Casodex (bicalutamide); CRPCa, castration resistant PCa; CSS, charcoal stripped serum; FACS, fluorescence-activated cell sorter; FRAP, fluorescence recovery after photobleaching, FRET, fluorescence resonance energy transfer; GR, glucocorticoid receptor; N/C interaction, amino- / carboxy- terminal interaction; OH-F, hydroxy-flutamide; PCa, prostate cancer; PR, progesterone receptor; PSA, prostate specific antigen; SA-β-Gal, senescence-associated β-galactosidase

Keywords: methyl anthranilate derivatives, antiandrogens, androgen receptor, antihormone, prostate cancer, cellular senescence

1. Introduction

PCa is the most diagnosed cancer in men. In the initial stage, the growth of PCa depends on androgens and the androgen receptor (AR) signaling [1, 2]. Therefore, blockage of androgen signaling is the central in hormone therapy. This includes the androgen deprivation therapy, which is combined with androgen antagonist (antiandrogen) treatment leading to the pharmacological reduction of androgen levels and blockage of the AR-signaling. At the beginning of the treatment, the lack of androgens leads to tumor regression. However, eventually during hormone therapy, PCa develops into a castration-resistant stage but remains AR-dependent [3, 4]. Inactivation of the AR also in castration-resistant PCa seems to be therefore a key target of treatment. Unfortunately, a therapy resistance may develop, which can be caused by mutations in exons coding for the AR ligand-binding domain (LBD) that can ultimately switch the action of antagonists into agonists. An example is the AR mutant T877A at which hydroxyflutamide (OH-F), a therapeutically used antiandrogen with strong AR inhibitory effect, acts as potent activator [5]. The AR T877A has been identified in PCa tumor samples from patients treated with OH-F. Other occurring AR mutants, such as AR-W741C or AR-F876L mediate resistance to bicalutamide and the second-generation antiandrogen enzalutamide, respectively [6, 7]. Therefore, identifying distinct mechanisms inhibiting the AR and AR mutants would be beneficial and interesting to obtain insights into structural requirements for AR antagonism. Thus, there is a need for new chemical platforms acting as AR antagonists.

The AR belongs to the subfamily of steroid receptors, which includes the glucocorticoid (GR) and progesterone receptors (PR). They all are members of the large nuclear receptor superfamily of ligand-inducible transcription factors. The AR consists of a carboxy- (C-) terminal LBD, a central DNA binding domain and the amino (N-)-terminus harboring the major transactivation function. Ligand binding induces the N/C terminal interaction of the AR. AR antagonists, so far analyzed, are able to inhibit this interaction [8, 9]. The androgen-activated AR rapidly translocates into the

nucleus and binds to chromatin and to DNA at hormone response elements to modulate gene expression [2]. Examples of direct AR target genes are *FKBP5* and the prostate-specific antigen (*PSA*/*KLK3*), which is an important diagnostic marker for PCa. AR may also repress some target genes such as maspin (*SERPINB5*) [10].

In our previous works, we identified and characterized novel steroidal AR antagonists based on the chemical platform of aminosteroids and dehydroepiandrosterones [11, 12] and also identified the first natural occurring AR antagonist atraric acid [13]. In the present work, we focused on the structural lead compound methyl anthranilate (MA) identified previously as an AR antagonist by analyzing saw palmetto extracts [15] and used here as a basis for a novel class of small molecular derivatives as selective AR antagonists. We analyzed in total 36 structural variants of MA, of which 23 compounds were synthesized. We carried out quantitative structure-activity relationships of AR antagonism in cellular assay systems using the androgen-dependent human PCa cell line LNCaP. Since clinically used AR antagonists are halogenated, effective halogen-substituted anthranilic acid esters were investigated in more detail for their mechanistic effects. Here, we identified a novel chemical platform that acts as a lead structure for new AR antagonists. This new chemical platform might be used in future for further optimization.

Therefore, we suggest that these novel antiandrogenic compounds may serve as a basis and chemical platforms for further analyses and designs in the context of structure-function relationship between ligands and the AR, also in terms of enhancing the diversity of AR antagonistic compounds that may be helpful for treating PCa in future.

2. Materials and methods

2.1. General methods for chemistry

The majority of synthesis were carried with modifications based on the reaction of isatoic anhydride with the respective alcohol as found by Georg Schmidt in 1887 and modified later by Staiger & Miller [14].

Melting points were determined with a heat table microscope HM-LUX (Leitz, Wetzlar, Germany) and are corrected. The NMR spectra were recorded on a JEOL ECA-500 spectrometer (500 or 400

MHz for ^{1}H and 125 or 100 MHz for ^{13}C) and referenced to the solvent resonances in $CDCl_3$ or acetone-d6 respectively. Chemical shifts are reported in ppm and are assigned as singlets (s), doublets (d), triplets (t), quartets (q), sextets, and multiplets (m); br abbreviates broad signal. The coupling constants (J) are reported as ^{1}J (direct coupling), ^{2}J (germinal coupling), ^{3}J (vicinal coupling) or ^{4}J (long-range coupling) in Hertz (Hz). The atom numberings of synthesized compounds are shown in supplementary Fig. 1. EI-MS and HR-EI-MS spectra were measured with a Micromass VG 7070H and a Micromass AutoSpec mass spectrometer using an ionizing energy of 70 eV.

Compound **18** and **19** were purified by preparative HPLC on a C18 reversed-phase column (Nucleodur C18 Gravity, 5 μm, ID 21 mm, L 250 mm; Macherey-Nagel, Düren, Germany) and isocratic elution with acetonitrile/water (70:30, v/v for compound **18**; 90:10, v/v for compound **19**) over 15 min at a flow rate of 22 mL/min. A Waters 990 diode-array detector was used for detection at λ= 254 nm.

The following compounds were purchased commercially: Methyl anthranilate (MA, **1**), methyl 2-pyrrol-1-ylbenzoate (**22**), methyl 2-amino-5-chloro-3-iodobenzoate (**28**), methyl 2-amino-4,5-methoxybenzoate (**29**), methyl-2-hydroxybenzoate (**37**) and methyl 2-(dimethylamino)benzoate (**20**) were purchased from Alfa Aesar (Ward Hill, MA, USA), methyl 4-aminopyridine-3-carboxylate (**33**) from Fluorochem (Derbyshire, UK). Phenyl 2-aminobenzoate (**15**), 2-amino-N-methylbenzamide (**24**) and methyl 2-aminothiophene-3-carboxylate (**32**), methyl 3-aminothiophene-2-carboxylate (**31**) and methyl 2-amino-5-chlorobenzoate (**26**) were purchased from ASDI Inc. (Newark, DE, USA). Methyl 2-amino-4-chlorobenzoate (**27**) and methyl 2-acetamidobenzoate (**23**) were purchased from Acros Organics (Thermo Fisher Scientific, Geel, Belgium), methyl 2-morpholino-4-yl-benzoate (**21**) from Maybridge (Cambridge, UK). The purity of each compound was ≥98 %.

2.2. Chemical synthesis

*2.2.1. Ethyl-2-aminobenzoate (**2**)*

Isatoic anhydride (4.08 g, 25 mmol) was dissolved in 40 mL ethanol and 0.05 g NaOH (1.25 mmol) was added. The mixture was heated at 65 °C until the gas generation had ceased, subsequently cooled and poured in 120 mL water. The product settled out as immiscible oil on the bottom. The oil was separated and distilled under vacuum over a 20 cm Vigreux column. The pure product, 2.99 g of a colorless oil (yield 72 %) passed over at 111 °C (5 Torr). ^{1}H NMR (500 MHz, $CDCl_3$) δ 1.38 (t, 3 H, ^{3}J= 7.2 Hz, 2'-H); 4.33 (q, 2H, ^{3}J= 7.2 Hz, 1'-H); 5.72 (br s, 2H, NH); 6.64 (m, 2H, 3-H, 5-H); 7.25 (m, 1H, 4-H); 7.88 (d, 1H, ^{3}J= 8.3 Hz, 6-H); ^{13}C NMR (100 MHz, $CDCl_3$) δ 14.4 (C2'); 60.4 (C1'); 111.2 (C1); 116.3 (C3); 116.8 (C5); 131.3 (C6); 134.1 (C4); 150.6 (C2); 168.3 (C7); EI-MS (70eV): m/z (rel. int.) = 165 [M+] (78), 137 (12), 119 (100), 92 (28), 65 (9); HR-EI-MS: m/z = 165.0776; $C_9H_{11}NO_2$ [M+] requires 165.0790.

*2.2.2. Propyl-2-aminobenzoate (**3**)*

Isatoic anhydride (4.08 g, 25 mmol) was dissolved in 40 mL 1-propanol and 0.05 g NaOH (1.25 mmol) was added. The mixture was heated at 65 °C until the gas generation had ceased, subsequently cooled and poured in 120 mL water. The product settled out as immiscible oil on the bottom. The oil was separated and distilled under vacuum over a 20 cm Vigreux column. The pure product, 3.28 g of a clear, slightly yellowish oil (yield 73 %) passed over at 130 °C (5 Torr). ^{1}H NMR (500 MHz, $CDCl_3$) δ 1.03 (t, 6 H, ^{3}J= 7.4 Hz, 3'-H); 1.78 (sextet, 2H, 2'-H); 4.23 (t, 2H, ^{3}J= 6.7 Hz, 1'-H); 5.73 (br s, 2H, NH); 6.64 (m, 2H, 3-H, 5-H); 7.25 (m, 1H, 4-H); 7.87 (d, 1H, ^{3}J= 8.0 Hz, 6-H); ^{13}C NMR (125 MHz, $CDCl_3$) δ 10.5 (C3'); 22.1 (C2'); 65.8 (C1'); 111.0 (C1); 116.3 (C3); 116.6 (C5); 131.1 (C6); 133.9 (C4); 150.4 (C2); 168.2 (C7); EI-MS (70eV): m/z (rel. int.) = 179 [M+] (61), 165 (29), 137 (25), 119 (100), 92 (24); HR-EI-MS: m/z = 179.0942; $C_{10}H_{13}NO_2$ [M+] requires 179.0945.

*2.2.3. Butyl-2-aminobenzoate (**4**)*

Isatoic anhydride (8.16 g, 50 mmol) was dissolved in 70 mL 1-butanol and 0.1 g NaOH (2.5 mmol) was added. The mixture was heated at 85 °C until the gas generation had ceased, subsequently cooled and poured in 120 mL water. The product settled out as immiscible oil on the bottom

together with remaining 1-butanol. The oil was separated and distilled under vacuum over a 20 cm Vigreux column. The pure product, 7.54 g of a clear, slightly yellowish oil (yield 78 %) passed over at 137.5 °C (5.5 Torr). ^{1}H NMR (500 MHz, $CDCl_3$) δ 0.97 (t, 3H, ^{3}J= 7.4 Hz, 4'-H); 1.47 (sextet, 2 H, 3'-H); 1.73 (quintet, 2H, 2'-H); 4.27 (t, 2H, ^{3}J= 6.6 Hz, 1'-H); 5.72 (br s, 2H, NH); 6.64 (m, 2H, 3-H, 5-H); 7.25 (dt, 1H, ^{3}J= 7.7 Hz, ^{4}J= 1.6 Hz, 4-H); 7.86 (dd, 1H, ^{3}J= 7.9 Hz, ^{4}J= 1.6 Hz, 6-H); ^{13}C NMR (125 MHz, $CDCl_3$) δ 13.8 (C4'); 19.4 (C3'); 30.9 (C2'); 64.3 (C1'); 111.2 (C1); 116.3 (C3); 116.8 (C5); 131.3 (C6); 134.0 (C4); 150.6 (C2); 168.2 (C7); EI-MS (70eV): m/z (rel. int.) = 193 [M+] (100), 137 (66), 119 (77), 92 (35), 65 (9); HR-EI-MS: m/z = 193.1103; $C_{11}H_{15}NO_2$ [M+] requires 193.1103.

*2.2.4. Pentyl-2-aminobenzoate (**5**)*

Isatoic anhydride (8.16 g, 50 mmol) was dissolved in 40 mL 1-pentanol and 0.1 g NaOH (2.5 mmol) was added. The mixture was heated at 85 °C until the gas generation had ceased, subsequently cooled and poured in 120 mL water. The product settled out as immiscible oil on the surface. The oil was separated and distilled under vacuum over a 20 cm Vigreux column. The pure product, 6.26 g of a colorless oil (yield 60 %) passed over at 147.5 °C (5 Torr). ^{1}H NMR (500 MHz, $CDCl_3$) δ 0.93 (t, 3H, ^{3}J= 7.0 Hz, 5'-H); 1.40 (m, 4 H, 3'-H, 4'-H); 1.76 (quintet, 2H, 2'-H); 4.26 (t, 2H, ^{3}J= 6.7 Hz, 1'-H); 5.72 (br s, 2H, NH); 6.64 (m, 2H, 3-H, 5-H); 7.25 (m, 1H, 4-H); 7.87 (d, 1H, ^{3}J= 8.3 Hz, 6-H); ^{13}C NMR (125 MHz, $CDCl_3$) δ 14.1 (C5'); 22.5 (C4'); 28.3 (C3'); 28.6 (C2'); 64.6 (C1'); 111.2 (C1); 116.3 (C3); 116.7 (C5); 131.3 (C6); 134.0 (C4); 150.6 (C2); 168.3 (C7); EI-MS (70eV): m/z (rel. int.) = 207 [M+] (100), 193 (6), 137 (66), 119 (75), 92 (21); HR-EI-MS: m/z = 207.1257; $C_{12}H_{17}NO_2$ [M+] requires 207.1259.

*2.2.5. Propan-2-yl-2-aminobenzoate (**6**)*

Isatoic anhydride (4.08 g, 25 mmol) was dissolved in 40 mL 2-propanol and 0.05 g NaOH (1.25 mmol) was added. The mixture was heated at 80 °C until the gas generation had ceased, subsequently cooled and poured in 120 mL water. The product settled out as immiscible oil on the bottom. The oil was separated and distilled under vacuum over a 20 cm Vigreux column. The pure

product, 2.45 g of a colorless oil (yield 55 %) passed over at 111 °C (0.7 Torr). ^{1}H NMR (500 MHz, $CDCl_3$) δ 1.35 (t, 6H, ^{3}J= 6.2 Hz, 1'-H, 3'-H); 5.21 (septet, 1H, ^{3}J= 6.2 Hz, 2'-H); 5.72 (br s, 2H, NH); 6.64 (m, 2H, 3-H, 5-H); 7.25 (m, 1H, 4-H); 7.87 (d, 1H, ^{3}J=8.2 Hz, 6-H); ^{13}C NMR (125 MHz, $CDCl_3$) δ 22.1 (C1', C3'); 67.7 (C2'); 111.6 (C1); 116.3 (C3); 116.7 (C5); 131.2 (C6); 133.8 (C4); 150.5 (C2); 167.8 (C7); EI-MS (70eV): m/z (rel. int.) = 179 [M+] (100), 137 (78), 119 (86), 92 (36), 65 (11); HR-EI-MS: m/z = 179.0942; $C_{10}H_{13}NO_2$ [M+] requires 179.0946.

*2.2.6. Butan-2-yl-2-aminobenzoate (**7**)*

Isatoic anhydride (4.08 g, 25 mmol) was dissolved in 40 mL 2-butanol and 0.05 g NaOH (1.25 mmol) was added. The mixture was heated at 100 °C until the gas generation had ceased, subsequently cooled and poured in 120 mL water. The product settled out as immiscible oil on the bottom. The oil was separated and distilled under vacuum over a 20 cm Vigreux column. The pure product, 2.53 g of a colorless oil (yield 52 %) passed over at 126 °C (5 Torr). ^{1}H NMR (500 MHz, $CDCl_3$) δ 0.97 (t, 3H, ^{3}J= 7.5 Hz, 4'-H); 1.32 (d, 3H, ^{3}J= 6.2 Hz, 1'-H); 1.61-1.79 (m, 2H, 3'-H); 5.06 (sextet, 1H, ^{3}J= 6.2 Hz, 2'-H); 5.72 (br s, 2H, NH); 6.64 (t, 2H, ^{3}J= 7.8 Hz, 3-H, 5-H); 7.25 (dt, 1H, ^{3}J= 7.4 Hz, ^{4}J= 1.9 Hz, 4-H); 7.87 (d, 1H, ^{3}J= 8.0 Hz, 6-H); ^{13}C NMR (125 MHz, $CDCl_3$) δ 9.7 (C4'); 19.6 (C1'); 28.9 (C3'); 72.1 (C2'); 111.5 (C1); 116.1 (C3); 116.6 (C5); 131.2 (C6); 133.8 (C4); 150.4 (C2); 167.8 (C7); EI-MS (70eV): m/z (rel. int.) = 193 [M+] (100), 179 (13), 137 (87), 119 (86); 92 (29); HR-EI-MS: m/z = 193.1108; $C_{11}H_{15}NO_2$ [M+] requires 193.1103.

*2.2.7. [(2S)-Butan-2-yl]-2-aminobenzoate (**8**)*

To a mixture of isatoic anhydride (1.59 g, 9.8 mmol) and 2-(s)-butanol (0.73 g, 9.8 mmol) dissolved in 10 mL 1,4-dioxane, NaOH was added (0.02 g, 0.5 mmol). The mixture was heated until moderate evolution of CO_2 gas occurred at approximately 90 °C. This temperature was maintained until gas evolution had ceased. After cooling, the reaction mixture was poured into 30 mL water, whereas a pale white precipitate was formed, which was filtered off and dried under vacuum. After drying it remained 1.21 g (yield 64 %) of a pale yellow oil as product. ^{1}H NMR (400 MHz, $CDCl_3$) δ 0.97 (t, 3H, ^{3}J= 7.5 Hz, 4-H); 1.32 (d, 3H, ^{3}J= 6.2 Hz, 1'-H); 1.55-1.78 (m, 2H, 3'-H); 5.05 (sextet, 1H, ^{3}J=

6.2 Hz, 2'-H); 5.72 (br s, 2H, NH); 6.64 (m, 2H, 3-H, 5-H); 7.25 (dt, 1H, ^{3}J= 7.4 Hz, ^{4}J= 1.6 Hz, 4-H); 7.87 (dd, 1H, ^{3}J= 8.0 Hz, ^{4}J= 1.6 Hz, 6-H); ^{13}C NMR (100 MHz, $CDCl_3$) δ 9.9 (C4'); 19.7 (C1'); 29.1 (C3'); 72.2 (C2'); 111.6 (C1); 116.3 (C3); 116.7 (C-5); 131.3 (C6); 133.9 (C4); 150.5 (C2); 167.9 (C7); EI-MS (70eV): m/z (rel. int.) = 207 [M+] (100), 151 (24), 137 (99), 92 (54); HR-EI-MS: m/z = 193.1088; $C_{11}H_{15}NO_2$ [M+] requires 193.1103.

*2.2.8. 3-Methylbutan-2-yl-2-aminobenzoate (**9**)*

To a mixture of isatoic anhydride (4.08 g, 25 mmol) and DL-3-methyl-2-butanol (2.20 g, 25 mmol) dissolved in 40 mL 1,4-dioxane, NaOH was added (0.05 g, 1.25 mmol). The mixture was heated at 100 °C under reflux for 12 h and subsequently poured into 120 mL water, where the product settled as immiscible oil. The oil was separated and distilled over a 20 cm Vigreux column, whereas the product, 4.01 g of a colorless oil (yield 77 %) passed over at 108-109 °C (0.8 Torr). ^{1}H NMR (400 MHz, $CDCl_3$) δ 0.99 (t, 6H, ^{3}J= 6.7 Hz, 4'-H, 5'-H); 1.27 (d, 3H, ^{3}J= 6.4 Hz, 1'-H); 1.91 (m, 1H, 3'-H); 4.95 (quintet, 1H, ^{3}J= 6.4 Hz, 2'-H); 5.73 (br s, 2H, NH); 6.64 (m, 2H, 3-H, 5-H); 7.25 (m, 1H, 4-H); 7.87 (d, 1H, ^{3}J= 8.0 Hz, 6-H); ^{13}C NMR (125 MHz, $CDCl_3$) δ 16.9 (C4'); 18.1 (C5'); 18.3 (C1'); 33.0 (C3'); 75.1 (C2'); 111.6 (C1); 116.3 (C3); 116.8 (C5); 131.2 (C6); 133.9 (C4); 150.6 (C2); 167.8 (C7); EI-MS (70eV): m/z (rel. int.) = 207 [M+] (100), 151 (24), 137 (99), 92 (54); HR-EI-MS: m/z = 207.1250; $C_{12}H_{17}NO_2$ [M+] requires 207.1259.

*2.2.9. 2-Methoxyethyl-2-aminobenzoate (**10**)*

Isatoic anhydride (8.16 g, 50 mmol) was dissolved in 60 mL 1,4-dioxane and 4.96 mL 1-methoxy-2-ethanol (50 mmol) and 0.1 g NaOH (2.5 mmol) were added. The mixture was heated at 110 °C until the gas generation had ceased, subsequently cooled and poured in 150 mL water. The product settled out as immiscible oil on the bottom. The oil was separated and distilled under vacuum over a 20 cm Vigreux column. The pure product, 6.29 g of a clear, slightly yellowish oil (yield 64 %) passed over at 136 °C (1 Torr). ^{1}H NMR (500 MHz, $CDCl_3$) δ 3.40 (s, 3H, 3'-H); 3.69 (t, 2H, ^{3}J= 4.8 Hz, 2'-H); 4.41 (t, 2H, ^{3}J= 4.8 Hz, 1'-H); 5.71 (br s, 2H, NH); 6.61 (m, 2H, 3-H, 5-H); 7.23 (m, 1H, 4-H); 7.88 (d, 1H, ^{3}J= 8.0 Hz, 6-H); ^{13}C NMR (125 MHz, $CDCl_3$) δ 58.9 (C3'); 63.2 (C2'); 70.5

(C1'); 110.5 (C1); 116.0 (C3); 116.5 (C5); 131.2 (C6); 134.0 (C4); 150.4 (C2); 167.9 (C7); EI-MS (70eV): m/z (rel. int.) = 195 [M+] (100), 137 (63), 120 (78), 92 (47); 59 (21); HR-EI-MS: m/z = 195.0898; $C_{10}H_{13}NO_3$ [M+] requires 195.0895.

*2.2.10. 3-Methoxypropyl-2-aminobenzoate (**11**)*

Isatoic anhydride (1.40 g, 8.6 mmol) was dissolved in 40 mL 1,4-dioxane and 0.772 g 3-methoxy-1-propanol (8.6 mmol) and 0.05 g NaOH (1.25 mmol) were added. The mixture was heated at 90 °C until the gas generation had ceased, subsequently cooled and poured in 120 mL water. The product settled out as immiscible oil on the bottom. The oil was separated and distilled under vacuum over a 20 cm Vigreux column. The pure product, 0.52 g of a yellowish oil (yield 29 %) passed over at 169 °C (2 Torr). ^{1}H NMR (500 MHz, $CDCl_3$) δ 2.02 (quintet, 2H, 2'-H); 3.35 (s, 3H, 4'-H); 3.53 (t, 2H, ^{3}J= 6.2 Hz, 3'-H); 4.36 (t, 2H, ^{3}J= 6.4 Hz, 1'-H); 5.71 (br s, 2H, NH); 6.64 (m, 2H, 3-H, 5-H); 7.25 (dt, 1H, ^{3}J= 7.6 Hz, ^{4}J= 1.6 Hz, 4-H); 7.85 (dd, 1H, ^{3}J= 8.0 Hz, ^{4}J= 1.6 Hz, 6-H); ^{13}C NMR (125 MHz, $CDCl_3$) δ 29.1 (C4'); 58.7 (C3'); 61.4 (C2'); 69.3 (C1'); 110.9 (C1); 116.2 (C3); 116.7 (C5); 131.2 (C6); 134.0 (C4); 150.5 (C2); 168.0 (C7); EI-MS (70eV): m/z (rel. int.) = 209 [M+] (100), 137 (65), 119 (72), 92 (32); 72 (26); HR-EI-MS: m/z = 209.1054; $C_{11}H_{15}NO_3$ [M+] requires 209.1052.

*2.2.11. 1-Methoxypropan-2-yl-2-aminobenzoate (**12**)*

Isatoic anhydride (8.16 g, 50 mmol) was dissolved in 60 mL 1,4-dioxane and 4.65 mL 1-methoxy-2-propanol (50 mmol) and 0.05 g NaOH (1.25 mmol) were added. The mixture was heated at 110 °C until the gas generation had ceased, subsequently cooled and poured in 150 mL water. The product settled out as immiscible oil on the bottom. The oil was separated and distilled under vacuum over a 20 cm Vigreux column. The pure product, 6.48 g of a clear, slightly yellowish oil (yield 62 %) passed over at 124-125 °C (0.4 Torr). ^{1}H NMR (500 MHz, $CDCl_3$) δ 1.34 (d, 3H, ^{3}J= 6.4 Hz, 1'-H); 3.39 (s, 3H, 4'-H); 3.48-3.60 (m, 2H, 3'-H); 5.29 (m, 1H, 2'-H); 5.71 (br s, 2H, NH); 6.63 (m, 2H, 3-H, 5-H); 7.24 (m, 1H, 4-H); 7.87 (dd, 1H, ^{3}J= 8.0 Hz, ^{4}J= 1.5 Hz, 6-H); ^{13}C NMR (125 MHz, $CDCl_3$) δ 16.8 (C1'); 59.2 (C4'); 69.2 (C2'); 75.2 (C3'); 111.1 (C1); 116.1 (C3); 116.3 (C5); 131.3

(C6); 134.0 (C4); 150.5 (C2); 167.5 (C7); EI-MS (70eV): m/z (rel. int.) = 209 [M+] (100), 137 (76), 120 (77), 92 (26); 73 (32); HR-EI-MS: m/z = 209.1044; $C_{11}H_{15}NO_3$ [M+] requires 209.1052.

*2.2.12. Cyclohexyl 2-aminobenzoate (**13**)*

To a mixture of isatoic anhydride (5.00 g, 31 mmol) and cyclohexanol (6.21 g, 62 mmol) dissolved in 40 mL 1,4-dioxane, NaOH (0.10 g, 2.5 mmol) was added. The mixture was heated under reflux for 12 h, subsequently cooled and poured in 120 mL water. The remaining solution was three times extracted with 100 mL diethyl ether and the combined organic phases were dried over Na_2SO_4. After removal of the diethyl ether, a reddish oil remained which was distilled under vacuum over a 20 cm Vigreux column. The pure product, 4.84 g of a pale yellow oil (yield 71 %) passed over at 145 °C (0.38 Torr). ^{1}H NMR (400 MHz, $CDCl_3$) δ 1.20-2.00 (m, 10 H, 2'-H, 3'-H, 4'-H, 5'-H, 6'-H); 5.00 (septet, 1H, 1'-H); 6.04 (br s, NH); 6.64 (m, 2H, 3-H, 5-H); 7.25 (dt, 1H, ^{3}J= 7.6 Hz, ^{4}J= 1.6 Hz, 4-H); 7.89 (dd, 1H, ^{3}J= 8.2 Hz, ^{4}J= 1.6 Hz, 6-H); ^{13}C NMR (100 MHz, $CDCl_3$) δ 23.8 (C3', C5'); 25.6 (C4'); 31.8 (C2', C6'); 72.4 (C1'); 111.7 (C1); 116.3 (C3); 116.8 (C5); 131.4 (C6); 134.0 (C4); 150.5 (C2); 167.1 (C7); EI-MS (70eV): m/z (rel. int.) = 219 [M+] (62), 137 (100), 119 (78), 92 (10); HR-EI-MS: m/z = 219.1245; $C_{13}H_{17}NO_2$ [M+] requires 219.1259.

*2.2.13. Cyclohexylmethyl 2-aminobenzoate (**14**)*

To a mixture of isatoic anhydride (5.00 g, 31 mmol) and cyclohexyl methanol (7.08 g, 62 mmol) dissolved in 35 mL 1,4-dioxane, NaOH was added (0.10 g, 2.5 mmol). The mixture was heated at 100 ºC under reflux for 12 h and subsequently poured into 120 mL water. The remaining solution was extracted three times with 100 mL diethyl ether and the combined organic phases were dried over Na_2SO_4. After evaporation of the diethyl ether, the remaining reddish oil was distilled under vacuum over a 20 cm Vigreux column. The product passed over at 152 °C (0.15 Torr). At room temperature, the product crystalized to give 6.42 g (yield 89 %) of a white powder. mp: 42-43 °C; ^{1}H NMR (400 MHz, $CDCl_3$) δ 1.06 (m, 2H, 4'-H_{ax}, 6'-H_{ax}); 1.24 (m, 3H, 4'-H_{eq}, 5'-H_{ax}, 6'-H_{ax}); 1.58-1.99 (m, 6H, 2'-H_{eq}, 3'-H, 5'-H_{eq}, 7'-H); 4.08 (d, 2H, ^{3}J= 6.4 Hz, 1'-H); 5.72 (br s, 2H, NH); 6.64 (m, 2H, 3-H, 5-H); 7.25 (dt, 1H, ^{3}J= 7.6 Hz, ^{4}J= 1.6 Hz, 4-H); 7.88 (dd, 1H, ^{3}J= 8.2 Hz, ^{4}J= 1.6

Hz, 6-H); ^{13}C NMR (100 MHz, $CDCl_3$) δ 25.9 (C4', C6'); 26.5 (C5'); 29.9 (C3', C7'); 37.4 (C2'); 69.5 (C1'); 111.1 (C1); 116.3 (C3); 116.8 (C5); 131.3 (C6); 134.1 (C4); 150.7 (C2); 168.3 (C7); EI-MS (70eV): m/z (rel. int.) = 233 [M+] (100), 137 (73), 119 (59), 92 (14); HR-EI-MS: m/z = 233.1415; $C_{14}H_{19}NO_2$ [M+] requires 233.1416.

*2.2.14. [(E)-3-Phenylprop-2-enyl]-2-aminobenzoate (**16**)*

Isatoic anhydride (9.00 g, 55 mmol) was dissolved in 70 mL 1,4-dioxane and 7.38 g cinnamyl alcohol (55 mmol) and 0.11 g NaOH (2.75 mmol) were added. The mixture was heated at 90 °C for 6 h, cooled and subsequently poured into 200 mL water. The product precipitated, was filtered off and recrystallized in methanol to give the pure product, 9.31 g of a pale yellow powder (yield 67 %). mp: 61 °C; ^{1}H NMR (500 MHz, $CDCl_3$) δ 4.94 (dd, 2H, ^{3}J= 6.3 Hz, ^{4}J= 1.4 Hz, 1'-H); 5.73 (br s, 2H, NH); 6.42 (m, 1 H, 2'-H); 6.65 (m, 2H, 3-H, 5-H); 6.73 (d, 1H, ^{3}J= 16.1 Hz, 3'-H); 7.24-7.44 (m, 6H, 4-H, 2''-H, 3''-H, 4''-H, 5''-H, 6''-H); 7.92 (d, 1H, ^{3}J= 8.2 Hz, 6-H); ^{13}C NMR (125 MHz, $CDCl_3$) δ 64.9 (C1'); 110.7 (C1); 116.3 (C3); 116.7 (C5); 123.6 (C1''); 126.6 (C2'', C6''); 128.0 (C2'); 128.6 (C3'', C5''); 131.3 (C6); 133.9 (C4''); 134.2 (C4); 136.3 (C3'); 150.6 (C2); 167.8 (C7); EI-MS (70eV): m/z (rel. int.) = 253 [M+] (63), 117 (100), 115 (16), 91 (8); HR-EI-MS: m/z = 253.1071; $C_{16}H_{15}NO_2$ [M+] requires 253.1103.

*2.2.15. Methyl-2-methylaminobenzoate (**17**)*

N-methylisatoic anhydride (5.0 g, 28 mmol) was dissolved in 40 mL methanol and 0.1 g NaOH (2.5 mmol) was added. The mixture was heated at 60 °C until the gas generation had ceased, subsequently cooled and poured in 120 mL water. The product settled out as immiscible oil on the bottom. The oil was separated and distilled under vacuum over a 20 cm Vigreux column. The pure product, 3.10 g of a clear, slightly yellowish oil (yield 67 %) passed over at 94 °C (1 Torr). ^{1}H NMR (500 MHz, $CDCl_3$) δ 2.91 (s, 3 H, 1''-H); 3.85 (s, 3H, 1'-H); 6.58 (m, 1H, 5-H); 6.66 (d, 1H, ^{3}J= 8.5 Hz, 3-H); 7.38 (dt, 1H, ^{3}J= 7.6 Hz, ^{4}J= 1.6 Hz, 4-H); 7.63 (br s, 1H, NH); 7.89 (dd, 1H, ^{3}J= 8.0 Hz, ^{4}J= 1.6 Hz, 6-H); ^{13}C NMR (100 MHz, $CDCl_3$) δ 29.6 (C1''); 51.5 (C1'); 109.9 (C1); 110.8 (C3); 114.4 (C5); 131.6 (C6); 134.7 (C4); 152.1 (C2); 169.2 (C7); EI-MS (70eV): m/z (rel. int.) =

165 [M+] (100), 132 (28), 119 (17), 105 (46), 40 (32); HR-EI-MS: m/z = 165.0792; $C_9H_{11}NO_2$ [M+] requires 165.0790.

*2.2.16. Methyl-2-ethylaminobenzoate (**18**)*

3.5 g NaOH (88 mmol) were suspended in 75 mL dimethylformamide (DMF) and a solution of 9.6 g isatoic anhydride (59 mmol) solved in 35 mL DMF was added at 30 °C dropwise over 30 min. Subsequently 7.2 mL ethyl iodide (88 mmol) were added dropwise over 20 min. The temperature never exceeded 44 °C. The mixture was stirred for 10 min and 50 mL methanol were added and subsequently stirred at 25 °C for 15 min. The methanol was evaporated and 200 mL water were added. The mixture was then extracted with hexane and washed several times with water. The hexane extract was evaporated and the remaining oil, distilled and subsequently purified by preparative HPLC to give the pure product, 1.78 g of a yellow oil (yield 17 %). ^{1}H NMR (500 MHz, $CDCl_3$) δ 1.31 (t, 3H, ^{3}J= 7.1 Hz, 2''-H); 3,23 (m, 2 H, ^{3}J= 7.1 Hz, 1''-H); 3.84 (s, 3H, 1'-H); 6.56 (m, 1H, 5-H); 6.68 (d, 1H, ^{3}J= 8.5 Hz, 3-H); 7.34 (m, 1H, 4-H); 7.59 (br s, 1H, NH); 7.89 (d, 1H, ^{3}J= 8.0 Hz, 6-H); ^{13}C NMR (125 MHz, $CDCl_3$) δ 14.5 (C2''); 37.4 (C1''); 51.4 (C1'); 109.6 (C1); 111.1 (C3); 114.2 (C5); 131.6 (C6); 134.6 (C4); 151.2 (C2); 169.1 (C7); EI-MS (70eV): m/z (rel. int.) = 179 [M+] (100), 164 (70), 146 (47), 132 (95), 119 (15); HR-EI-MS: m/z = 179.0956; $C_{10}H_{13}NO_2$ [M+] requires 179.0946.

*2.2.17. Methyl-2-propylaminobenzoate (**19**)*

3.5 g NaOH (88 mmol) were suspended in 75 mL dimethylformamide (DMF) and a solution of 9.6 g isatoic anhydride (59 mmol) solved in 35 mL DMF was added at 30 °C dropwise over 30 min. Subsequently 8.05 mL 1-bromopropane (88 mmol) were added dropwise over 20 min. The temperature never exceeded 44 °C. The mixture was stirred for 10 min and 50 mL methanol were added and subsequently stirred at 25°C for 15 min. The methanol was evaporated and 200 mL water were added. The mixture was then extracted with hexane and washed several times with water. The hexane extract was evaporated and the remaining oil, distilled and subsequently purified by preparative HPLC to give the pure product, 1.47 g of a yellow oil (yield 13 %). ^{1}H NMR (500

MHz, $CDCl_3$) δ 1.03 (t, 3H, ^3J= 7.3 Hz, 3''-H); 1.71 (sextet, 2H, ^3J= 7.3 Hz, 2''-H); 3.16 (q, 2 H, ^3J= 6.2 Hz, 1''-H); 3.85 (s, 3H, 1'-H); 6.56 (m, 1H, 5-H); 6.68 (d, 1H, ^3J= 8.5 Hz, 3-H); 7.34 (m, 1H, 4-H); 7.70 (br s, 1H, NH); 7.89 (d, 1H, ^3J= 8.0 Hz, 6-H); ^{13}C NMR (125 MHz, $CDCl_3$) δ 11.7 (C3''); 22.4 (C2''); 44.6 (C1''); 51.4 (C1'); 109.6 (C1); 111.1 (C3); 114.1 (C5); 131.6 (C6); 134.5 (C4); 151.3 (C2); 169.1 (C7); EI-MS (70eV): m/z (rel. int.) = 193 [M+] (91), 164 (85), 132 (100), 119 (27), 105 (11); HR-EI-MS: m/z = 193.1191; $C_{11}H_{15}NO_2$ [M+] requires 193.1103.

*2.2.18. 2-[(2-Aminobenzoyl)amino]benzoic acid (**25**)*

Isatoic anhydride (2.5 g, 15 mmol) and anthranilic acid (2.3 g, 17 mmol) were suspended in 50 mL water. The mixture was heated at 100 °C for 4 h. After cooling, crystals were formed which were filtered off and washed with water. The product, pale yellow acicular crystals were purified by recrystallization in ethanol/chloroform (50:50) to give 2.92 g of pure product (yield 76 %). mp: 201-202 °C; ^{1}H NMR (400 MHz, acetone-D6) δ 2.82 (br s, 2H, NH); 6.62-7.76 (m, 6H, 3-H, 4-H, 5-H, 6-H, 4'-H, 5'-H); 8.15 (dd, 1H, ^3J= 8.0 Hz, ^4J= 1.6 Hz, 6'-H); 8.87 (dd, 1H, ^3J= 8.6 Hz, ^4J= 1.1 Hz, 3'-H); 12.04 (s, 1H, NH); ^{13}C NMR (400 MHz, acetone-D6) δ 115.0 (C1); 115.6 (C2'); 117.4 (C3); 117.5 (C5); 120.0 (C6'); 122.2 (C4'); 127.5 (C3'); 131.5 (C6); 132.8 (C5'); 134.6 (C4); 142.6 (C1'); 151.1 (C2); 168.0 (C7); 170.0 (C7'); EI-MS (70eV): m/z (rel. int.) = 256 [M+] (100), 238 (16), 120 (82), 92 (17); HR-EI-MS: m/z = 256.0818; $C_{14}H_{12}N_2O_3$ [M+] requires 256.0848.

*2.2.19. Methyl 2-amino-4-(trifluoromethyl)benzoate (**30**)*

2-amino-4-(trifluoromethyl)benzoic acid (0.50 g, 2.44 mmol) was dissolved in 40 mL methanol and 8 mL HClc were added slowly. The mixture was stirred and heated under reflux for 12 h. Subsequently, the methanol was evaporated and the remaining residue suspended in water. This mixture was adjusted to an alkaline pH by adding a 10 % NaOH solution and extracted with diethyl ether. The combined organic phases were dried over Na_2SO_4. After evaporation of the diethyl ether, the remaining solid was recrystalized in isohexane to give 0.50 g (yield 93 %) of a yellowish powder. mp: 62 °C; ^{1}H NMR (400 MHz, $CDCl_3$) δ 3.89 (s, 3H, 1'-H); 5.90 (br s, 2H, NH); 6.84 (dd, 1H, ^3J= 8.2 Hz, ^4J= 1.6 Hz, 5-H); 6.89 (s, 1H, 3-H); 7.94 (dd, 1H, ^3J= 8.2 Hz, ^4J= 1.6 Hz, 6-H); ^{13}C

NMR (100 MHz, $CDCl_3$) δ 52.0 (C1'); 112.4 (q, ^3J (C,F)= 3.8 Hz, C3); 113.1 (C1); 113.5 (q, ^3J (C,F)= 4.8 Hz, C5); 123.6 (q, ^1J (C,F)= 273.2 Hz, C8); 132.2 (C6); 135.5 (q, ^2J (C,F)= 31.6 Hz, C4); 150.3 (C2); 113.1 (C1); 167.8 (C7); EI-MS (70eV): m/z (rel. int.) = 219 [M+] (100), 200 (25), 187 (91), 160 (81); HR-EI-MS: m/z = 219.0507; $C_9H_8F_3NO_2$ [M+] requires 219.0494.

*2.2.20. Butan-2-yl-2-amino-4-(trifluoromethyl)benzoate (**30a**)*

2-amino-4-(trifluoromethyl)benzoic acid (0.50 g, 2.44 mmol) was dissolved in 40 mL *sec*-butanol and 8 mL concentrated HCl were added slowly. The mixture was stirred and heated under reflux for 12 h. Subsequently, the *sec*-butanol was evaporated and the remaining residue suspended in water. This mixture was adjusted to an alkaline pH by adding a 10 % NaOH solution and extracted with diethyl ether. The combined organic phases were washed with water and subsequently dried over Na_2SO_4. After evaporation of the diethyl ether, it remained 0.17 g (yield 27 %) of an orange colored oil as product. ^{1}H NMR (400 MHz, $CDCl_3$) δ 0.96 (t, 3H, ^3J= 7.4 Hz, 4'-H); 1.33 (d, 3H, ^3J= 6.2 Hz, 1'-H); 1.60-1.81 (m, 2H, 3'-H); 5.07 (sextet, 1H, ^3J= 6.2 Hz, 2'-H); 5.91 (br s, 2H, NH); 6.83 (dd, 1H, ^3J= 8.2 Hz, ^4J= 1.2 Hz, 5-H); 6.89 (s, 1H, 3-H); 7.96 (d, 1H, ^3J= 8.2 Hz, 6-H); ^{13}C NMR (100 MHz, $CDCl_3$) δ 9.8 (C4'); 19.6 (C1'); 29.0 (C3'); 72.9 (C2'); 112.3 (q, ^3J (C,F)= 3.8 Hz, C3); 113.5 (q, ^3J (C,F)= 3.8 Hz, C5); 113.9 (C1); 123.7 (q, ^1J (C,F)= 273.1 Hz, C8); 132.2 (C6); 135.5 (q, ^2J (C,F)= 31.7 Hz, C4); 150.3 (C2); 167.8 (C7); EI-MS (70eV): m/z (rel. int.) = 261 [M+] (61), 239 (48), 205 (100), 187 (99); HR-EI-MS: m/z = 261.0977; $C_{12}H_{14}F_3NO_2$ [M+] requires 261.0947.

*2.2.21. Methyl 3-aminonaphthalene-2-carboxylate (**34**)*

3-Amino-2-naphthoic acid (1.00 g, 0.5 mmol) was slowly added to a mixture of 15 mL H_2SO_4c and 30 mL methanol and allowed to react for 5 h under reflux. During this time another mixture of methanol/H_2SO_4c (35 mL/10 mL) was gradually added. After cooling, the reaction mixture was stirred another 12 h at room temperature, subsequently evaporated and the remaining solution was poured on ice. When neutralizing with saturated Na_3CO_3 solution, a yellow precipitate was formed which was filtered off, solved in dichlormethane and washed several times with water. After drying of the organic phase over Na_2SO_4, the solvent was removed and 0.62 g (yield 61 %) of pure product

remained. mp: 97-98 °C; ^{1}H NMR (400 MHz, $CDCl_3$) δ 3.95 (s, 3H, 1'-H); 5.61 (br s, 2H, NH); 6.97 (s, 1H, 3-H); 7.18 (m, 1H, 6-H); 7.40 (m, 1H, 7-H); 7.52 (d, 1H, ^{3}J= 8.2 Hz, 5-H); 7.71 (d, 1H, ^{3}J= 8.5 Hz, 8-H), 8.49 (s, 1H, 10-H); ^{13}C NMR (100 MHz, $CDCl_3$) δ 52.0 (C1'); 110.1 (C3); 114.8 (C1); 122.6 (C7); 125.2 (C5); 126.1 (C9); 128.9 (C6); 129.3 (C8); 133.5 (C10); 137.4 (C4); 146.1 (C2); 168.4 (C11); EI-MS (70eV): m/z (rel. int.) = 201 [M+] (100), 169 (73), 142 (45), 115 (17); HR-EI-MS: m/z = 201.0790; $C_{12}H_{11}NO_2$ [M+] requires 201.0789.

*2.2.22. Methyl-3-aminobenzoate (**35**)*

3-Aminobenzoic acid (5.48 g, 40 mmol) was dissolved in 60 mL methanol and 4.36 mL thionyl chloride (60 mmol) were added dropwise with stirring and cooling on ice. When the reaction had stopped, the methanol was evaporated and the remaining residue was neutralized with saturated $NaHCO_3$ solution and extensively extracted with ethyl acetate. After evaporation of the ethyl acetate, a reddish oil remained which was distilled under vacuum over a 20 cm Vigreux column. The pure product passed over at 118 °C (0.3 Torr) and crystalized by cooling to give 5.46 g of a white powder (yield 90 %). mp: 31-32 °C; ^{1}H NMR (500 MHz, $CDCl_3$) δ 3.82 (br s, 2H, NH); 3.87 (s, 3H, 1'-H); 6.84 (d, 1H, ^{3}J= 8.4 Hz, 4-H); 7.19 (m, 1H, 5-H); 7.34 (s, 1H, 2-H); 7.40 (d, 1H, ^{3}J= 7.5 Hz, 6-H); ^{13}C NMR (100 MHz, $CDCl_3$) δ 51.9 (C1'); 115.6 (C2); 119.3 (C4); 119.5 (C6); 129.1 (C5); 131.0 (C1); 146.5 (C3); 167.2 (C7); EI-MS (70eV): m/z (rel. int.) = 151 [M+] (100), 120 (72), 92 (45), 65 (13).

*2.2.23. Methyl-4-aminobenzoate (**36**)*

4-Aminobenzoic acid (2.74 g, 20 mmol) was dissolved in 30 mL methanol and 2.18 mL thionyl chloride (30 mmol) were added dropwise with stirring and cooling on ice. When the reaction had stopped, the methanol was evaporated and the remaining residue was neutralized with saturated $NaHCO_3$ solution and extensively extracted with ethyl acetate. The organic phase was dried over Na_2SO_4 and subsequently evaporated. The pure product remained, 2.60 g of slightly yellowish acicular crystals (yield 86 %). mp: 107-108 °C ^{1}H NMR (500 MHz, $CDCl_3$) δ 3.85 (s, 3H, 1'-H); 4.04 (br s, 2H, NH); 6.64 (d, 2H, ^{3}J= 8.7 Hz, 3-H, 5-H); 7.85 (d, 2H, ^{3}J= 8.7 Hz, 2-H, 6-H); ^{13}C

NMR (100 MHz, $CDCl_3$) δ 51.6 (C1'); 113.8 (C3, C5); 119.8 (C1); 131.6 (C2, C6); 150.8 (C4); 167.1 (C7); EI-MS (70eV): m/z (rel. int.) = 151 [M+] (92), 120 (100), 92 (23), 65 (10).

2.3. Cell culture and functional analysis of derivatives

Monkey kidney CV-1 and COS-7 cells lacking endogenous functional steroid receptors as well as HeLa cells were maintained in Dulbecco´s modified Eagle´s medium (DMEM), supplemented with 10 % (v/v) fetal calf serum (FCS) (Invitrogen) and penicillin (100 IU/mL), and streptomycin (100 IU/mL) at 37°C and 5 % CO_2. The androgend dependent PCa cell line LNCaP was cultured in (RPMI), supplemented with 10 % (v/v) FCS, 1 % (v/v) sodium pyruvate and penicillin (100 IU/mL), and streptomycin (100 IU/mL) at 37°C and 5 % CO_2. For growth assays 5 % FCS was used. Hep3B cells stably expressing GFP-AR-wt or YFP-AR-CFP were cultured in α-MEM (Lonza) supplemented with 5 % FCS, 2 mM L-glutamine, 100 U/mL penicillin, 100 µg/mL streptomycin and 600 µg/mL G418.

The plasmid pMMTV-luc, which contains a luciferase reporter gene driven by the mouse mammary tumor virus long terminal repeats that is responsive to androgens [15]. The expression vectors for the human AR, pSG5-hAR, pSG-hAR T877A, W741C, GR and PR have been described earlier [9][16]. The expression vector for AR-F876L was kindly provided by Dr. Charles Sawyers. For the transfection experiments, CV-1 cells were seeded onto 6-well tissue culture plates (Greiner Bio-One, Germany) at 10^5 cells per well, and grown in DMEM supplemented with 10 % (v/v) charcoal-stripped serum [17]. Six hours later, cells were transfected using the $CaPO_4$-method essentially as described earlier [17]. The DNA mixture per well for transfections consisted of 1 µg of the MMTV-luciferase reporter construct, 0.2 µg of the pSG5-hAR expression vector, and 0.2 µg of the cytomegalovirus (CMV)-driven β-galactosidase expression vector (pCMV-lacZ), which was used as an internal control for transfection efficiency. After 14 hours, media were replaced either with or without the addition of androgens together with the indicated compounds. After additional 48 hours, cells were lysed and assayed for luciferase and β-galactosidase activity. Obtained luciferase units were normalized to those obtained with β-galactosidase. All transfection assays shown were

performed in duplicate and were repeated at least three times. Growth analyses were performed as described previously [13].

2.4. Whole-cell binding assay

The competitive whole-cell binding assay using tritium-labeled mibolerone has been described elsewhere,[13] and was used here with one modification: COS-7 cells were transfected using the $CaPO_4$-method with 0.75 µg of the pSG5-hARwt plasmid, together with 0.2 µg of the pCMV-lacZ expression vector for normalization/control per well.

2.5. Real time RT-PCR

The reverse transcription quantitative real-time PCR (RT-qPCR) was performed essentially as described previously with specific primers for detection of PSA, FKBP5 and maspin mRNA and β-actin mRNA for normalization for the indicated cell via the ΔΔCt method using CFX manager software from Bio-Rad.[13] As modifications 2 x 10^5 cells were seeded out directly in media containing 10 % charcoal stripped FCS. After two days cells were treated with the indicated compounds or solvent (DMSO) or androgen (R1881 100 pM). RNA was isolated from the cells using peqGOLD TriFast (Peqlab, Erlangen, Germany) according to the manufacturer's protocol. One-step RT-qPCR was conducted using the SuperScript™ III One-Step RT-PCR System with Platinum™ Taq DNA Polymerase kit (Invitrogen, Carlsbad, USA), gene specific primers and Biorad CFX96™ Real Time PCR detection system. RT-qPCR results were analyzed via ΔΔCt method using CFX manager software from Bio-Rad.

2.6. Detection of the SA-β-galactosidase

Senescence-associated β-galactosidase (SA-β-gal) staining was carried out as described previously[18, 19] using 40,000 cells per well in a 6-well plate. The treatment was performed for three days. The percentage of stained cells was determined following counting at least 400 cells per well under a light microscope.

2.7. FACS, FRET and FRAP assays

FACS analyses were performed as described earlier.[16] Acceptor photobleaching FRET and FRAP assays were performed as described earlier.[16]

2.8. Translocation studies

AR nuclear translocation studies were performed in general as described earlier.[20] As modification the transfected cells were treated for 90 min with the first indicated compound and additional 90 min with either androgen (R1881 100 pM) or DMSO as solvent control, resulting in an overall incubation time of 180 min. Further for specific translocation analysis the protein biosynthesis inhibitor cycloheximide (50 µg/mL) was added to all dishes at the beginning of the treatment.

3. Results

3.2. Quantitative structure-activity relationship analysis.

Previously we identified MA (compound **1**) to be a potent inhibitor of the AR [15]. In order to further characterize this lead structure, we synthesized and analyzed derivatives of MA with different structural modifications. To detect specific antiandrogenic potential we used the established AR-dependent reporter gene assay using CV1 cells that lack endogenous AR as well as the closely related GR and PR, which could potentially interfere with the assay system. The cells were cotransfected with an expression vector encoding the AR-wt and the androgen-responsive promoter-luciferase reporter (pMMTV-luc). Cells were treated with the indicated compounds either alone to analyze their role in activating the AR, or together with the specific synthetic AR agonist R1881 to analyze AR antagonism of the derivatives (Fig. 1; see the Supporting Information for details). Treatment with DMSO alone was used as solvent control. Antagonistic activity of the tested compounds resulted in reduced AR-mediated transactivation induced by androgen treatment. Within this test system, a repression of the activating effect of R1881 is equivalent to the AR inhibitory potential of the tested compound.

We observed that an elongation of the alkyl ester chain strongly increased the inhibitory effect upon the androgen receptor (Fig. 1A). At a compound concentration of 300 µM, the addition of one methylene group (-CH_2-) to the ester chain increased the repression of the androgenic effect from 8.7-fold (compound **1**) to about 35-fold (compound **2**) and the addition of a propyl, butyl, or pentyl group to more than 53-fold (compound **3**, **4, 5**).

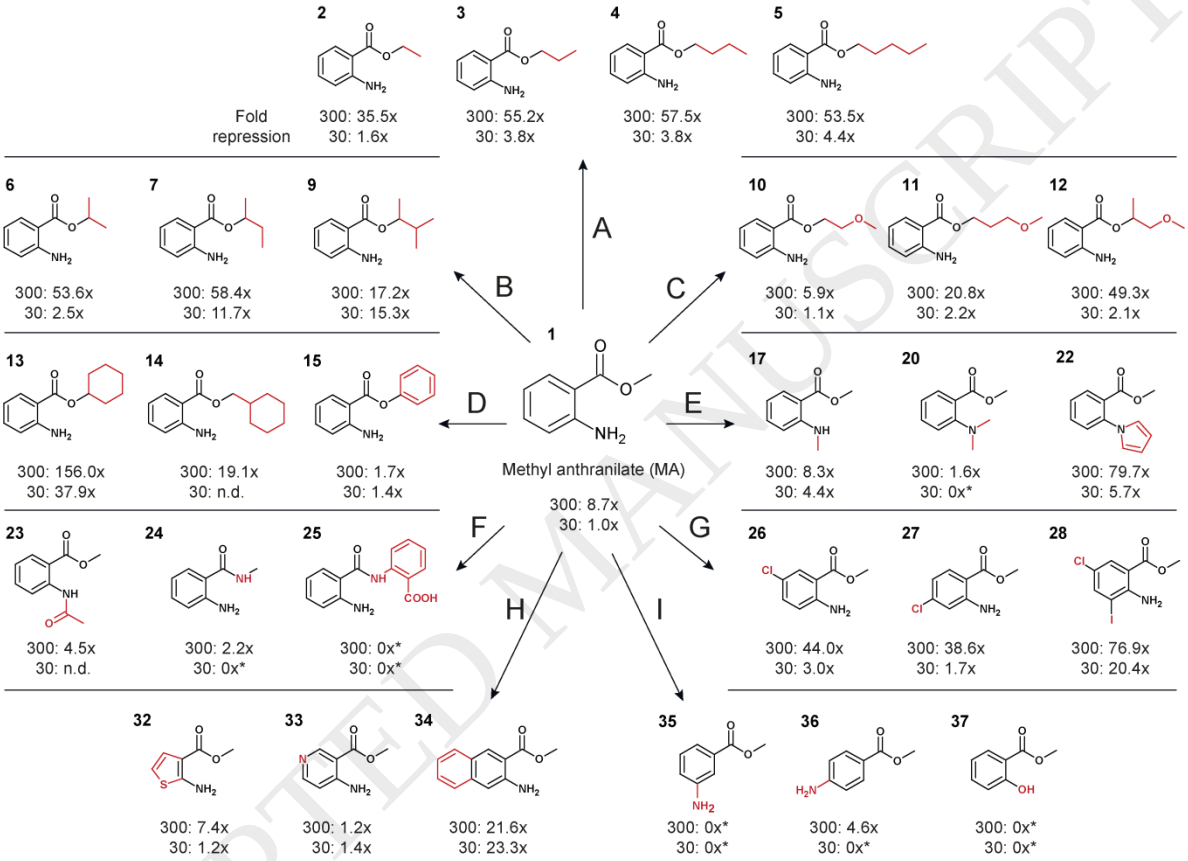

Fig. 1. Schematic overview of tested structural changes in the lead structure methyl-anthranilate (MA, compound **1**). Modified derivatives (structural changes labeled in red) were tested for their inhibitory effect upon the AR in an androgen receptor dependent MMTV-luc reporter gene assays using CV-1 cells lacking endogenous AR as well as the closely related GR and PR, which could potentially interfere with the assay system. The fold repression of compound concentrations of 300 µM (300) and 30 µM (30) were calculated by correlating normalized relative light units (RLU) of treated and untreated cells (Supplemental Fig. 3) in the presence or absence of the synthetic androgen R1881 (30 pM). Fold repression indicates the maximum potential of each compound to repress the androgenic effect of R1881. (A) Unbranched alkyl esters. (B) Branched alkyl esters. (C) Alkoxy esters. (D) Esters with ring structure. (E) Modifications of the amino group. (F) Derivatives with amide group. (G) Halogen substitutions at the benzene ring. (H) Variations of the ring system. (I) Shifting of the amino group and exchange to hydroxyl group. n.d.: not determined. *negative inhibition values were set as 0x repression.

The introduction of brunched alkyl ester groups also led to a stronger repression of the androgenic effect of R1881 (compound **6** and **8**, Fig. 1B and Supplemental Fig. 2). At a concentration of 30 µM, compound **7** led to ~11-fold repression, which is about 10-fold stronger compared to the lead structure **1**, compound **9** even led to a 15.3-fold repression. However, at lower concentrations (30 µM) the antiandrogenic potential of compounds **2** to **6** converged to those of the lead structure (Fig. 1A and B).

Adding oxygen atoms to the ester chain, to receive alkoxy esters (Fig. 1C), led also to an increase of the AR antagonism. At 300 µM, compounds **10** to **12** showed a strong repression of the R1881-mediated AR activation, although, when compared to similar structures without oxygen atoms (Fig. 1A and B), the repression effect was decreased and nearly vanished using 30 µM of the compounds.

Flexible six-carbon ring structures in the ester group (Fig. 1D) increased the repression of the effect of R1881 (compound **13** and **14**) at 300 µM compared to the leading structure **1**, but the additional methylene group in compound **14** led to a sharp decline when compared to compound **13**. The addition of a rigid benzene ring structure, such as phenyl (compound **15**) or cinnamoyl (compound **16**, Supplemental Fig. 2) led to a strong decrease of repression being tantamount to the AR inhibitory effect.

Changing the amino group in the leading structure **1** to a secondary amine as N-methyl derivative (compound **17**, Fig. 1E), seemed to increase the AR inhibitory potency slightly at 30 µM concentration, however, an elongation of the alkyl chain to ethyl or propyl (compound **18** and **19**, Supplemental Fig. 2) lowered the effect. A change to a tertiary amine (compound **20**) strongly reduced the antiandrogenic effect, but integrating the amino group as tertiary amine into a ring structure such as pyrrole (compound **22**) or morpholine (compound **21**, Supplemental Fig. 2) led to increased AR inhibition.

The introduction of amido groups into the lead structure **1** (Fig. 1F) resulted in a decrease of AR inhibition (compound **23** and **24**). Moreover, adding a rigid space-consuming benzene ring with substituted carboxy group resulted in a total loss of the AR inhibitory potential (compound **25**).

Halogen substitution at the benzene ring (-Cl or -I) of the lead structure **1** (Fig. 1G) strongly increased the AR inhibitory effect. Therefore, we focused on these derivatives since halogenated compounds are also used as clinically used as antiandrogens, such as OH-F. By comparison of mono chlorine substituted derivatives at concentrations of 300 and 30 µM (compound **26** and **27**), it became apparent that a halogen substitution in meta position to the carbonyl group is leading to a stronger repression of the androgenic effect of R1881 than substitution at the para position. A derivative with halogens at both meta positions to the carbonyl group showed a stronger effect (compound **28**) than the derivate with only one halogen at the meta position (compound **26**). Substitutions at the benzene ring with two methoxy groups or a trifluoromethyl group (compound **29** and **30**, Supplemental Fig. 2) only slightly increased AR inhibition. Extending the hydrophobic side chain, compound **30a,** enhanced AR antagonism.

Exchanging the benzene ring in the lead structure **1** (Fig. 1H) to a thiophene (compound **32** and compound **31**, Supplemental Fig. 2) decreased the AR inhibition compared to the lead compound. A change to a pyridine ring (compound **33**) almost led to a loss of the AR inhibitory potential. Adding an annulated saturated ring system to give a naphthalene derivative (compound **34**), showed a strong increase in repression of the R1881-mediated AR transactivation.

To investigate the influence of the amino group in the lead structure, derivatives with different substitution position of the amino group and an exchange of the amino group to a hydroxyl group were tested (Fig. 1I). Shifting the amino group from ortho in meta position (compound **35**) resulted in a total loss of the AR inhibitory effect, a shift to the para position (compound **36**) led to a strong decrease. Also, the replacement of the amino group with a hydroxyl group resulted in a total loss of AR inhibitory potential (compound **37**).

3.3. Halogen-substituted compounds inhibit the androgen-activated AR mutants that mediate resistance to current clinically used AR antagonists.

Halogen-substituted anthranilic acid esters (compounds **26**, **27**, **28** (Fig. 1G) including compounds **30**, **30a**, Supplemental Fig. 2) revealed throughout and consistently high levels of AR antagonistic activity as shown above. Therefore, we chose this group for further mechanistical investigation at

the molecular level in comparison to the lead structure compound **1**. In addition, these compounds contain some structural similarities to clinically applied antiandrogens such as hydroxyflutamide (OH-F).

Even though the synthetic R1881 is preferentially used in cell culture experiments, since it is less metabolized compared to the natural androgen dihydrotestosterone (DHT), it had to be clarified whether the compounds can also inhibit the DHT-activated AR. This is important since the AR conformational change is dependent on the bound ligand and might therefore alter possible subsequent antiandrogenic effects. Similar results compared to the R1881-activated AR were obtained in the presence of DHT (supplementary Fig. 4A). Further, we tested whether the halogen-substituted anthranilic acid esters can also inhibit the AR-T877A mutant. This AR mutant is often expressed in resistant PCa tumors [5] and confers resistance to OH-F treatment. Comparing the inhibitory potential of the compounds towards the AR-wt and the AR-T877A suggests a distinct pattern of inhibition. While compound **28** inhibits most potently the AR-wt, the compound **30a** is more efficiently in inhibiting AR-T877A (Fig. 2A). Interestingly this effect is independent of the used AR-agonist, since we obtained similar results with the DHT-activated AR-T877A mutant (supplementary Fig. 4B). The AR-F876L mutant confers resistance to the second generation AR antagonist enzalutamide [6]. Analyzing this AR mutant in the same experimental setup, the halogenated compounds inhibited the AR-F878L mediated transactivation, whereas enzalutamide activated this receptor mutant using each 30 µM of compounds (Fig. 2B). Compound **28** appeared to be the most effective inhibitor of AR-F876L. To include also bicalutamide resistance AR mutant (AR-W741C) and to compare the activity of compound **28** with enzalutamide and bicalutamide with AR mutants 10 µM of each compound was used (Fig. 2C and supplementary Fig. 5). The data suggest that compound **28** inhibits not only wild-type but also the AR-mutants AR-T877A, AR-F876L, and AR-W741C. This indicates that compound **28** exhibits a different molecular mechanism of AR antagonism compared to enzalutamide and bicalutamide.

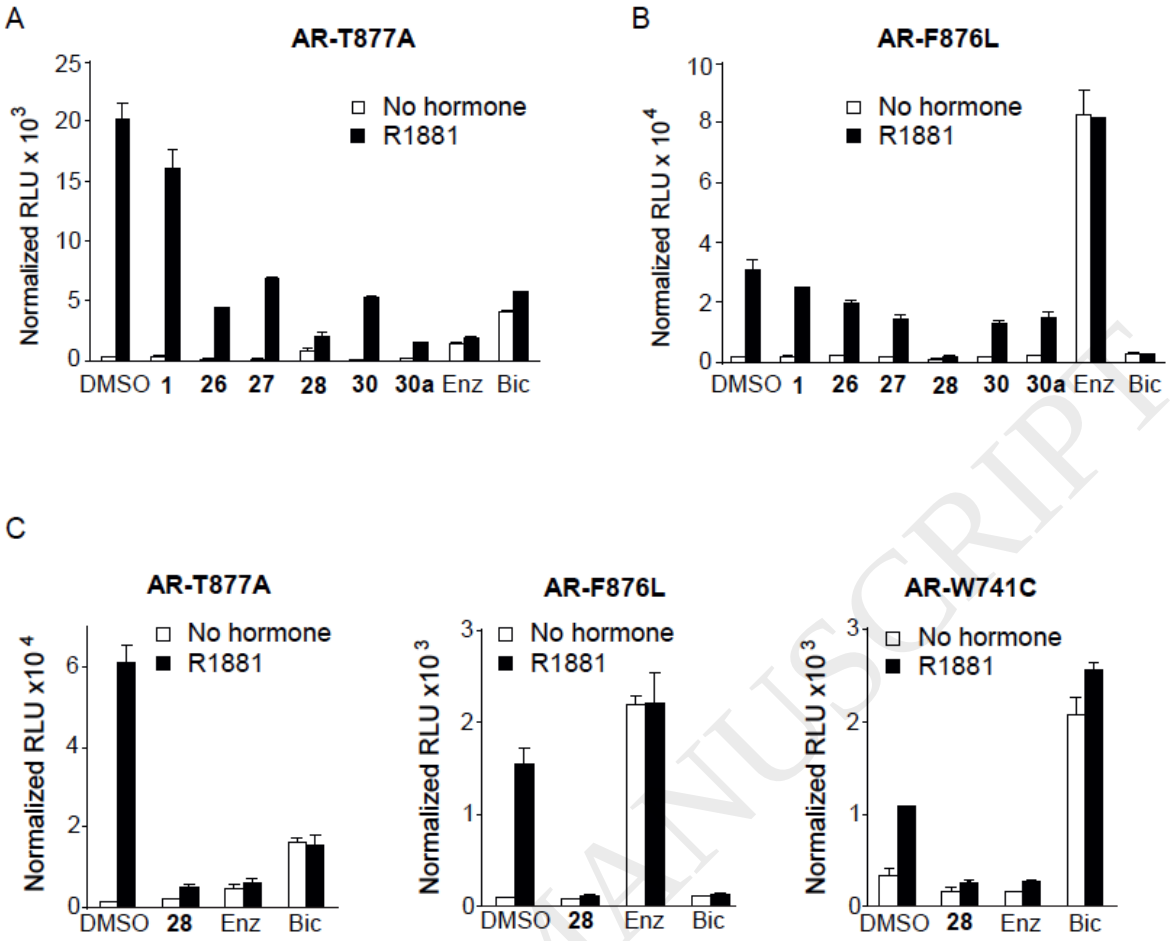

Fig. 2. Halogen-substituted anthranilic acid esters reduce the transactivation of the AR-T877A mutant. Similar experimental setup of reporter assays as described in Fig. 1 using the expression vectors for the AR mutants or AR-T877A, AR-F876L, and AR-W741C in the presence of R1881 (30 pM). Compounds were applied in 30 µM (A) and (B) or 10 µM (C) final concentration. Results represent luciferase activity normalized to β-galactosidase activity derived from the co-transfected pCMV-lacZ vector. Error bars show standard deviation of the mean. Enz, enzalutamide; Bic bicalutamide.

3.4. Lack of inhibition of the GR and PR by halogen-substituted MA-derivatives

To determine receptor specificity, we tested whether compound **26**, **27**, **28**, **30** or **30a** effect the closely AR-related nuclear receptors GR and PR. Similar experimental setups as for AR were used including the MMTV-luc reporter. Transfected cells with expression vectors for the GR or PR were treated with the glucocorticoid dexamethasone or progesterone, respectively. Interestingly, we did neither observe antagonism nor agonism by the compounds for either GR or PR suggesting that the compounds are AR-specific antagonists (Fig. 3).

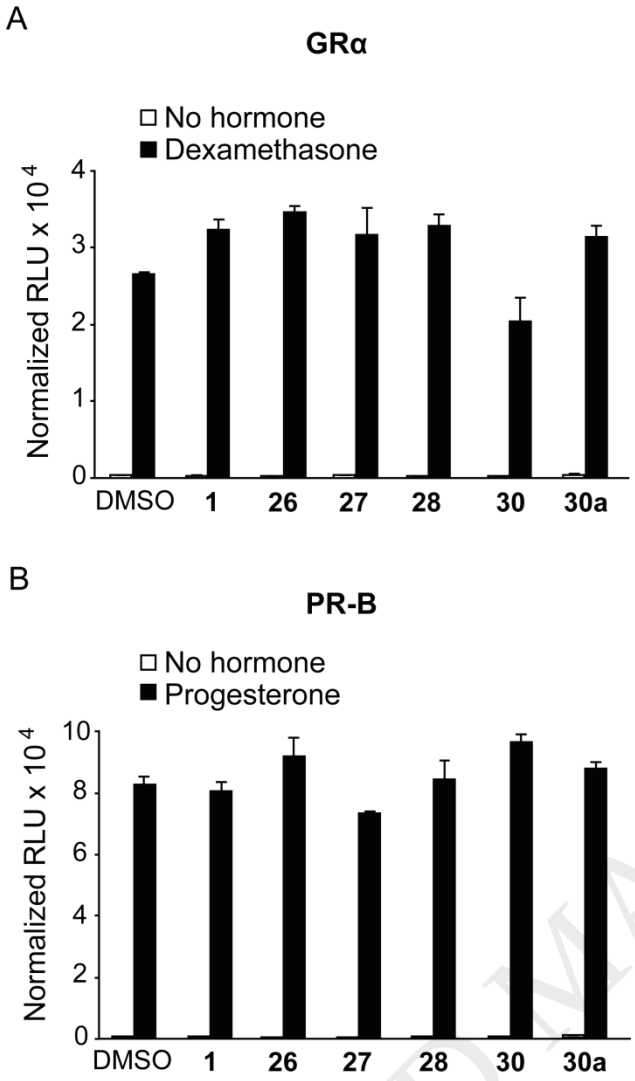

Fig. 3. Halogen-substituted anthranilic acid esters do not affect glucocorticoid- (GR) or progesterone- (PR) mediated transactivation. Similar experimental setup of reporter assays as described in Figure 1 using (A) the transcriptional active human GRα or (B) the PR-B expression vector and the designated agonists dexamethasone (10 nM) or progesterone (10 nM), respectively. Compounds were applied in 30 µM final concentration. Error bars show standard deviation of the mean.

3.5. Inhibition of endogenous AR target gene expression

To investigate whether the chosen compounds affect the expression of endogenous AR target genes, RT-qPCR was performed. We detected mRNA levels of the androgen-induced target genes *PSA* and *FKBP5* and the androgen repressed gene maspin (*SERPINB5*) in human PCa LNCaP cells, which endogenously express the AR-T877A mutant. As expected, both PSA and FKBP5 mRNA levels were increased upon treatment with androgen (Fig. 4A and B) whereas, the maspin mRNA levels

were reduced (Fig. 4C). The tested compounds inhibited the androgen-induced PSA and FKBP5 mRNA levels while compound **1** and compounds **27**, **28** and **30** abolished the androgen-mediated repression of maspin mRNA levels.

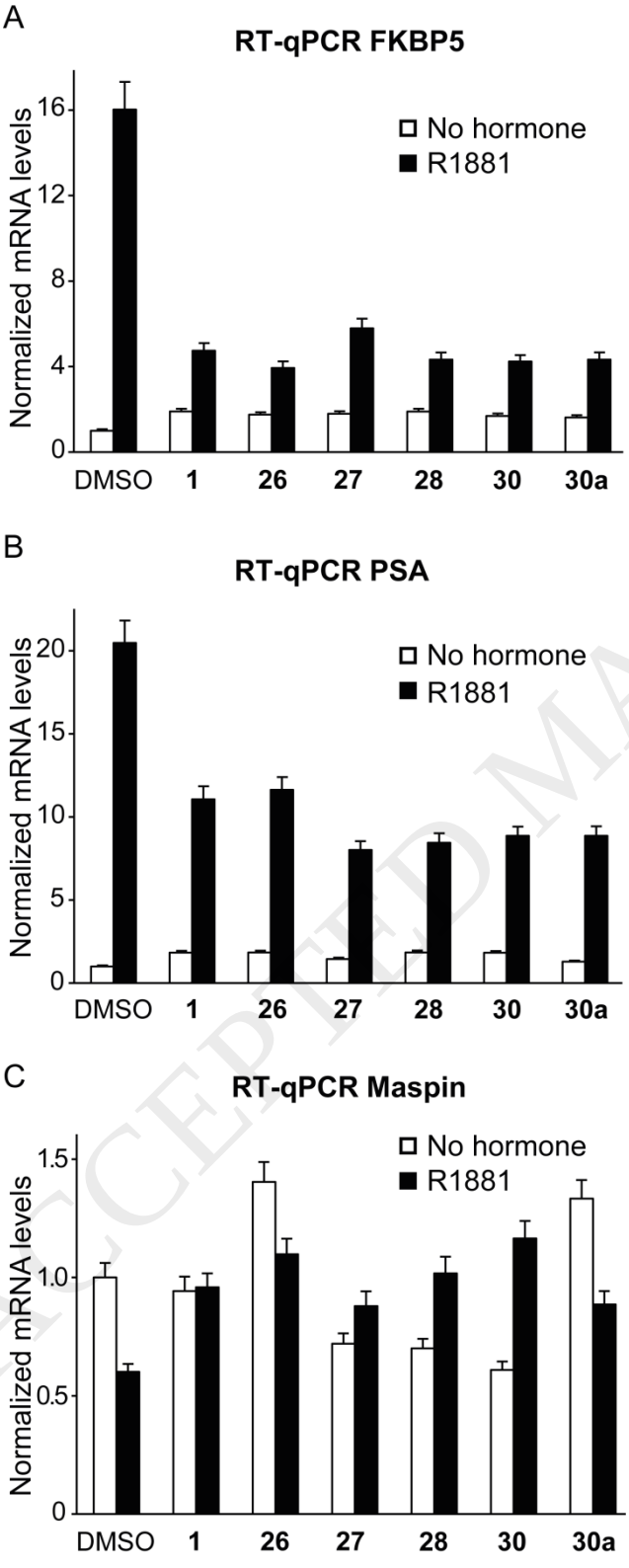

Fig. 4. Inhibition of endogenous AR induced target genes in LNCaP cells by halogen-substituted anthranilic acid esters. Relative mRNA expression was determined by RT-qPCR. Cells were treated of indicated compounds with or without the addition of R1881 (100 pM). Compounds were applied in 30 µM final concentration except 1 had a final concentration of 300 µM. Whole RNA was isolated and analyzed by RT-qPCR. Results show normalized fold expression of the mRNA of the androgen-regulated genes (A) *FKBP5*, (B) *PSA* (*KLK3*) and (C) maspin (*SERPINB2*) normalized to β-actin and relative to DMSO control (solvent control). Error bars show standard deviation of the mean.

3.6. Halogen-substituted anthranilic acid esters require the AR-LBD for AR-binding

Next, we tested whether halogen-substituted anthranilic acid esters require the AR-LBD for AR inhibition applying an AR mutant lacking the LBD (ARΔLBD) (Fig. 5A). This mutant is known to be transcriptionally active in the absence of androgens. The analyzed compounds did not inhibit the AR-mediated transactivation, indicating that these compounds act through the LBD of the AR.

To further confirm binding of the compounds to the AR, whole-cell binding assays with the compounds **26**, **27**, **28**, **30** and **30a** were performed (Fig. 5B). The obtained results suggest that **1** and the halogenated anthranilic acid ester derivatives compete for androgen binding and further indicate that these compounds bind to the LBD of AR. Our results reveal that for the action of **1** and the tested derivatives the AR LBD is crucial.

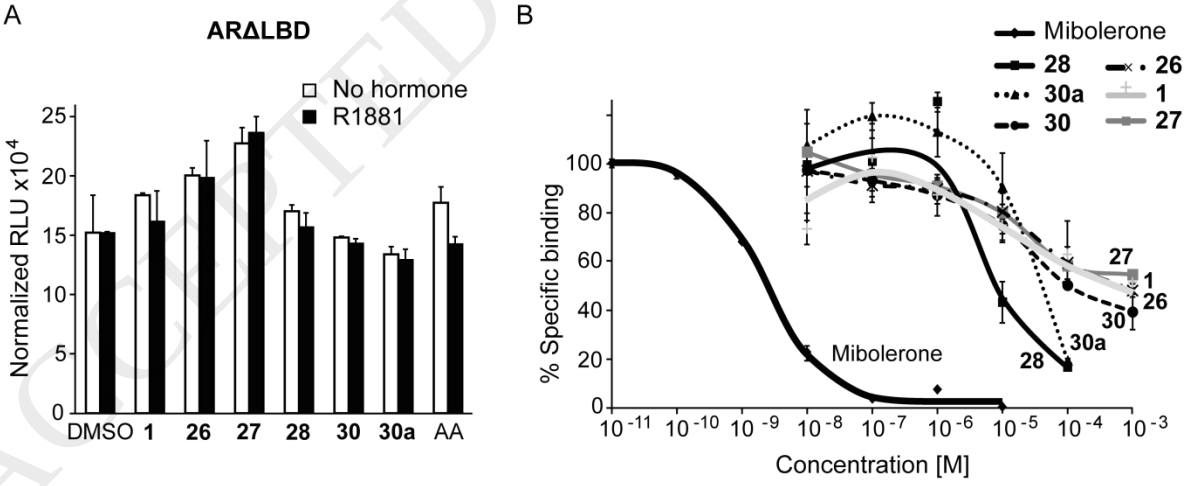

Fig. 5. Halogen-substituted anthranilic acid esters require the AR-LBD for antagonism and compete for androgen binding to the AR. (A) The activity of the constitutively nuclear localized ARΔLBD, which lacks the ligand-binding domain (LBD), was tested in reporter assays as described in Fig. 1. Error bars show standard deviation of the mean. (B) Competitive whole-cell binding assays were performed using pSG5-hAR-wt transfected COS-7 cells co-incubated with 1 nM ^{3}(H)-mibolerone in the absence or presence of increasing concentrations of either unlabeled mibolerone or the indicated compounds for 90 min. Competition for

binding is measured as disintegrations per unit time (dpm) normalized with an internal transfection control using the β-galactosidase activity derived from co-transfected pCMV-lacZ vector and illustrated as percentage of specific binding. Results are averages of triplicates with error bars as standard deviations of the mean. Reduced dpm suggest competition for ligand binding.

3.7. Halogen-substituted MA-derivatives inhibit cell proliferation of human PCa cells.

To address whether the inhibition of AR-mediated transactivation coincides with inhibition of cell proliferation, we treated human androgen-dependent growing LNCaP cells with the indicated compounds (Fig. 6). Interestingly, the treatment with all tested compounds led to a reduced growth of LNCaP cells (Fig. 6A).

To analyze the underlying mechanism of growth inhibition, we explored the activity of senescence-associated β-galactosidase (SA-β Gal) activity, a specific marker for cellular senescence in which cells irreversibly arrest in the G1/G0 cell cycle phase. We observed that the expression of SA-β Gal activity was induced to various degrees in treated cells (Fig. 6B). The efficacy of inhibition of LNCaP cell growth by compounds **26** and **28** correlated with a higher induction of SA-β Gal activity. In line with this, the FACS data suggest a higher number of cells in the G1/G0-phase when treated with **28** without an increase in the SubG1-phase, suggesting that apoptosis is not induced (Fig. 6C). Our data indicate that the compounds inhibit cell proliferation, the cell cycle and are able to induce cellular senescence.

Since compounds **26** and **28** had similar activities and acted AR specifically, we focused on compound **28** for further investigations.

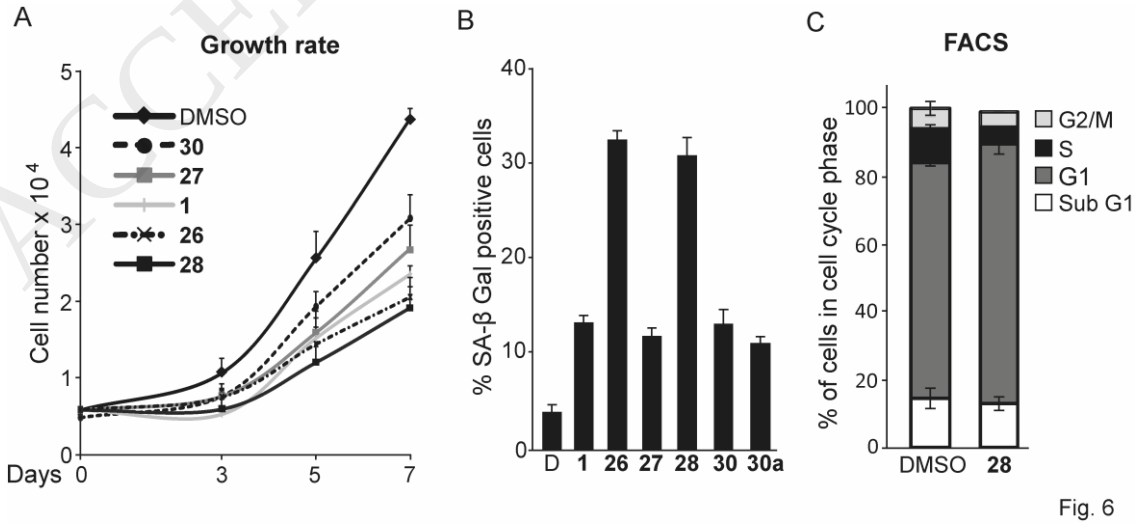

Fig. 6

Fig. 6. Halogen-substituted anthranilic acid esters inhibit the growth of LNCaP cells and induce cellular senescence. (A) Growth curve analysis of LNCaP cells treated with the indicated compounds (30 μM). Cells were cultured in medium supplemented with 5 % FCS. From day three on cells were trypsinized and counted or medium change including compound treatment was performed every second day. Values show means and standard deviation of four values. DMSO was used as solvent control. (B) The assay for the induction of cellular senescence in LNCaP cells was performed by treatment with the indicated compounds (30 μM) for three days. The cells were fixed and stained for senescence-associated (SA)-β-galactosidase. Subsequently cells were counted under a light microscope. Results show relative amounts of stained cells and are presented as mean of two wells +SD. (C) FACS analysis were performed to analyze the cell cycle state of cells. LNCaP cells were incubated for 72 h with solvent control DMSO or compound **28** (30 μM), fixed with ethanol and stained with propidium iodide followed by cytometric analysis. Counts of the different cell cycle phases are presented in percent.

3.8. Compound 28 inhibits the nuclear translocation, N/C interaction and increases nuclear mobility of the AR

To address whether the nuclear translocation of the AR is affected, the intracellular distribution of the AR was determined after indicated times in the presence or absence of androgens in living HeLa cells, transiently transfected with a GFP-AR expression vector (Fig. 7A). Expectedly, the data show that androgen treatment leads to a potent nuclear translocation with the majority of the GFP-AR signals detected in the nuclei. Treatment with compound **28** also induced nuclear translocation of AR, however, to a much weaker extent, revealing that binding of **28** to AR leads to only a weak nuclear translocation. Co-treatment of R1881 with **28** showed reduced nuclear GFP-signals compared to treatment with androgen alone suggesting that the androgen-induced nuclear localization is reduced (Fig. 7A).

Besides nuclear translocation, androgen binding to the AR also induces the interaction between the N-terminal domain of the AR and the cofactor binding groove in the C-terminal LBD (N/C-interaction) that is considered to play an important role in AR dimerization, controls co-regulator binding and is important for full AR activation [20-23]. To analyze whether the N/C-interaction induced by the synthetic androgen R1881 is modulated through compound **28**, double-tagged AR (YFP–AR–CFP) was assessed using acceptor photobleaching FRET (fluorescence resonance energy transfer) assays (Fig. 7B). The data suggest that compared to the previously shown antiandrogenic

spiro-oxetan-steroids,[12] the here described compound **28** might induce slightly the N/C interaction and in line with this, co-treatment with compound **28** does not significantly reduce the R1881 induced FRET between the AR termini.

Binding of androgens to the AR results in a strongly reduced nuclear mobility and transient immobilization of AR in the nucleus due to stable chromatin and DNA binding [24, 25], probably due to accumulation of receptors at sites of transcription [22]. Therefore, to further test the hypothesis whether AR mobility might be changed by AR binding, compound **28** was used in FRAP (fluorescence recovery after photobleaching) experiments (Fig. 7C). The data suggest that after photobleaching the redistribution of fluorescence in the presence of R1881 is much slower compared to compound **28**. Simultaneous treatment of R1881 and **28** resulted also in a faster AR nuclear mobility compared to agonist alone indicating that compound **28** inhibits chromatin association/ DNA binding of the AR. This is in line with our observation that, in contrast to other antagonists, we did not observe the binding of the co-repressors SMRT, NCoR or Alien to the AR in the presence of **28** in mammalian two hybrid system experiments (data not shown). These results suggest that compound **28** decreases nuclear translocation, increases the nuclear AR mobility, and thus indicates a reduction of androgen-mediated stable chromatin and/or DNA binding of the AR.

Taken together, halogenated anthranilic acid ester derivatives exhibit androgen receptor antagonism without interruption of the AR N/C interaction.

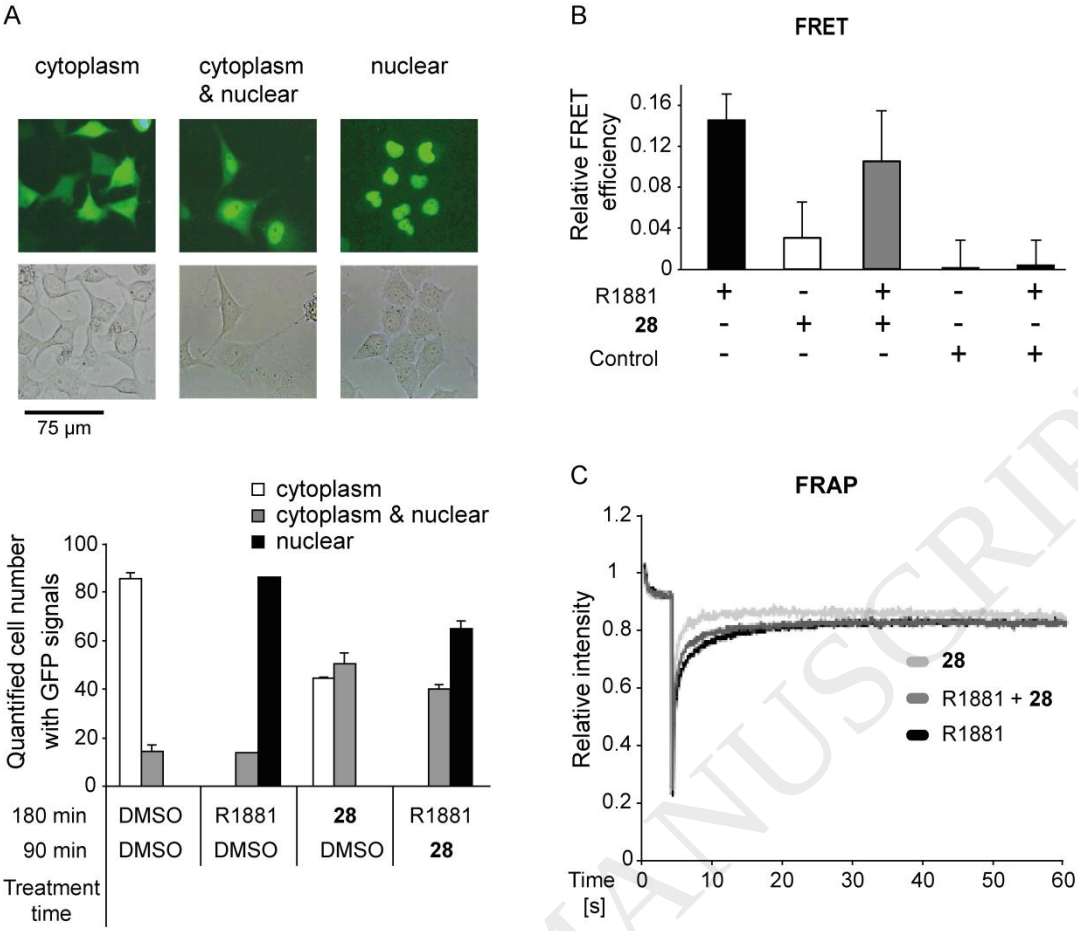

Fig. 7. Compound **28** inhibits the nuclear AR translocation and enhances the intranuclear mobility of the AR. (A) Fluorescence microscopy and phase contrast images of transiently transfected HeLa cells expressing GFP-AR in the absence or presence of R1881 (100 pM) or compound **28** (30 µM) in medium containing charcoal treated FCS. Upper panel: For analysis, three categories of intracellular GFP signals as counting criteria were used: "cytoplasm", mixed "cytoplasm and nuclear," as well as "nuclear". Lower Panel: Quantitative analysis with the counted number of GFP positive cells sorted in one of the three categories. DMSO was used as solvent control. First indicated substance row depicts a total treatment time of 180 min, whereas within this period, after 90 min, the second indicated substance was additionally added. (B) Fluorescence resonance energy transfer (FRET) assays were used to analyze the AR N/C interaction with an acceptor photobleaching in living cells. Hep3B cells stably expressing double-tagged AR (YFP-AR-CFP) were cultured for 24 h in medium containing charcoal treated FCS with the indicated compounds (R1881 (100 pM), **28** (30 µM)) or, as a control, the previously described AR-antagonist spiro-oxetan-steroid.[12] Values for the treated samples represent the average +SEM of at least 40 cells measured in three independent experiments. (C) FRAP assays indicate the intranuclear mobility of GFP-AR using wild-type AR in living cells. In strip-FRAP measurements, fluorescent molecules in a narrow strip spanning the nucleus were bleached for 100 ms at maximum laser power. Subsequently, fluorescence in the strip was monitored every 100 ms. Fluorescence intensities were plotted against time and normalized to the pre-bleach value. Mean values of at least 40 cells measured in three independent experiments are plotted. A faster increase of fluorescence intensity after photobleaching indicates higher protein mobility (R1881 (100 pM), **28** (30 µM)).

4. Discussion

Here, we identified a new chemical platform as a structural lead compound and analyzed the structure-antagonism relationships of anthranilate derivatives. We have previously shown that steroidal derivatives, particularly aminosteroid derivatives, can act as potent AR inhibitors [11]. Also, steroids based on spiro-oxolan and spiro-oxetan may serve as a good basis to design AR antagonists that specifically antagonize the transactivation of the AR [12]. Potent non-steroidal molecules are clinically used as AR-specific antagonists. Among those, bicalutamide shows structural similarities to enzalutamide (MDV3100), a next generation AR antagonist used for hormone therapy of castration resistant PCa [26]. These compounds are composed of two benzene rings connected in a chain-like structure and are halogen-substituted with a characteristic trifluoromethyl group. Interestingly, OH-F also contains a trifluoromethyl group substituted at the benzene ring. However, when we introduced a trifluoromethyl group at the benzene ring in selected compounds (compare **1** with **30** or compounds **7** with **30a**) no change of the level of AR antagonism was observed. Nevertheless, some halogenated derivatives are more effective within the group of halogenated derivatives (compound **26** to **28**, Fig. 1E) as compared to **1**. Interestingly, when we added amido groups, which are a part of the structures of OH-F or bicalutamide, to our lead structure (compound **23** to **25**), we found a strong decrease of the antiandrogenic effect compared to **1**. This might suggest that these novel compounds described here interact by a different mode with the AR.

Mutations of the AR occur in PCa and mediate resistances to the therapy. For example, the AR-T877A mutant cannot be inhibited by OH-F and in fact this AR mutant is even activated by treatment with OH-F. Similarly, AR mutants AR-F876L and AR-W741C mediate resistance towards enzalutamide and bicalutamide, respectively [6]. In the present study, halogenated MA-derivatives, particular compound **28**, inhibits all these three AR mutants, which indicates a distinct mode of inhibition of AR-mediated transactivation. Compound **30**, which also contains a trifluoromethyl group, but has slightly different substituents compared to OH-F, is able to inhibit the OH-F resistant AR-T877A mutant, showing that only minor changes in the structure can decide if

the compound is able to inhibit OH-F resistant AR mutants. Therefore, there is a need to provide novel and diverse types of AR antagonists for future individualized treatment. Small molecules consisting of a central benzene ring with distinct substituents seem to be the basis for very effective antiandrogens.

By investigating the structure-activity relationships of the lead structure MA (compound **1**) we identified different parts of the structure to be important for exerting an inhibition of the AR. The scaffold of MA is formed by a benzoic ester with an amino group in ortho position. We showed previously that the change of the ester to a carboxy acid group, to give anthranilic acid, led to a remarkable reduction of the antiandrogenic effect [15], underlining the importance of the ester group in the lead structure. Exchanging the amino group or shifting the amino group to another position of the benzene ring results in a loss of antiandrogenic potential. When replacing the benzene ring by a 5-ring (thiophene) or 6-ring (pyridine) heterocycles, the AR inhibitory effect decreased. These findings lead to the conclusion that the scaffold of a benzoic ester with amino group in ortho position is essential to exert a strong antiandrogenic effect.

An elongation of the unbranched ester alkyl group or branched alkyl ester groups increased the AR inhibitory potential. Ring systems in the ester group are only effective when they are flexible, inflexible rings reduce the antiandrogenic effect. The strongest increase in antiandrogenic potential can be achieved by adding halogen substituents at the meta position to the carbonyl group.

When changing the ester moiety to a phenyl ester (compound **15**) no potent AR antagonism was seen whereas a flexible saturated cyclohexyl ring (compounds **13** and **14**), acts as potent AR antagonist. A possible explanation would be that the phenyl ring is planar and rigid whereas the saturated cyclohexyl ring is not planar and flexible, which may lead to a different interaction with amino acids of the AR-LBD. These data suggest that compounds with minor chemical modifications might be useful to synthesize and analyze in order to obtain insights into the effects of side chains important for AR antagonism.

Focusing on substitutions of the benzene ring of compound **1**, we found that halogen-substituted anthranilic acid ester derivatives bind to the AR, inhibit androgen-induced transactivation, androgen-induced gene expression of endogenous AR target genes, cell proliferation and exhibit AR

specific antagonism.

Comparing the effect on AR-mediated transactivation of compound **1** to compound **26** and **27**, it became obvious that substitution with only one halogen at the benzene ring is sufficient to strongly enhance the AR antagonism. Compound **28** with two halogen substitutions inhibited even more potently the androgen-induced transactivation and reduced cell proliferation.

On cellular level, proliferation assays, cytometric analysis of cell cycle as well as SA-β Gal staining data suggest that treatment with compound **28** inhibits cell proliferation and induces cellular senescence in androgen-dependent growing LNCaP cells. Cellular senescence is a program that arrests cells irreversibly in the G1/G0 cell cycle phase. Even though the induction of cellular senescence was observed upon compound **28** treatment, not all cells underwent this cellular program. In line with this, we did not observe a complete growth arrest, which indicates that non-senescent cells were able to grow. Nevertheless, the induction of cellular senescence by a compound that inhibits both AR-mediated transactivation and chromatin and DNA recruitment indicates that the antagonist-bound AR is not a pure inactivated AR but harbors cellular functions. Therefore we speculate that the induction of cellular senescence might occur at a different level. Our previous studies that analyzed the natural compound atraric acid indicate that the Src-Akt factors are involved in AR antagonist-induced cellular senescence [8, 9].

On molecular level, treatment with **28** leads to a decreased nuclear translocation and FRAP analyses indicate that **28** increases the intranuclear mobility of the AR, suggesting that the stable androgen-induced chromatin/DNA binding is inhibited. This proposes an underlying molecular reason, namely that AR target gene expression and AR signaling is reduced by compound **28**. Interestingly, in contrast to many AR antagonists that inhibit the N/C-interaction of the AR [8, 9], compound **28** seems not to inhibit the N/C interaction induced by androgens although compound **28** inhibits AR-mediated transactivation and competes with androgens for binding to the AR. This further supports the notion concept that compound **28** acts at molecular level in a different manner to inhibit the AR compared to other known AR-antagonists. It also suggests that the lack of inhibition of the N/C interaction is not necessary for AR antagonism. Thus, screening assays based on inhibition of the AR N/C interaction will exclude the identification of compounds that act similar to compound **28**.

Conclusions

The compounds described in the present study on one hand differ chemically from recent clinically used AR antagonists and on the other hand exhibit a different molecular mechanism to inhibit the AR. The scope of this manuscript is to emphasize that a novel chemical platform has been identified that acts as a lead structure for new AR antagonists. The new compounds inhibit not only wildtype but also those AR mutants that mediate resistance to flutamide, bicalutamide, or enzalutamide. This indicates a novel AR-ligand interaction, which could of interest for analyses of receptor-ligand interaction with subsequent altered function. Furthermore, the compounds induce cellular senescence despite inhibition AR-mediated transactivation indicating a non-genomic activity. This new chemical platform might be used for further optimization and analyses of additional derivatives with more potent AR antagonistic effect. Future analyses should investigate more detailed the effect of different halogen substituents at different positions of the lead structure and combine AR antagonistic effect-increasing structural elements as described in this study.

Thus, the novel small molecule antagonists may serve as novel chemical platforms for new types of AR antagonists to enhance the spectrum and diversity of currently available AR antagonists that act additionally against distinct AR mutants.

Acknowledgements and Funding

The expression vector for AR-F876L was kindly provided by Dr. Charles Sawyers. This work was supported by the German Cancer Aid foundation (A.B.) and Boehringer Ingelheim Fonds (W.H.). This work was also supported by the Federal Ministry of Education and Research (BMBF), Germany, and FKZ: 01EO1002 (A.B.H.).

References

[1] C.J. Ryan, D.J. Tindall, Androgen receptor rediscovered: the new biology and targeting the androgen receptor therapeutically, Journal of clinical oncology : official journal of the American Society of Clinical Oncology, 29 (2011) 3651-3658.

[2] T. Matsumoto, M. Sakari, M. Okada, A. Yokoyama, S. Takahashi, A. Kouzmenko, S. Kato, The androgen receptor in health and disease, Annu Rev Physiol, 75 (2013) 201-224.

[3] R.B. Marques, N.F. Dits, S. Erkens-Schulze, W.M. van Weerden, G. Jenster, Bypass mechanisms of the androgen receptor pathway in therapy-resistant prostate cancer cell models, PloS one, 5 (2010) e13500.

[4] S. Perner, M.V. Cronauer, A.J. Schrader, H. Klocker, Z. Culig, A. Baniahmad, Adaptive responses of androgen receptor signaling in castration-resistant prostate cancer, Oncotarget, 6 (2015) 35542-35555.

[5] M.E. Taplin, G.J. Bubley, Y.J. Ko, E.J. Small, M. Upton, B. Rajeshkumar, S.P. Balk, Selection for androgen receptor mutations in prostate cancers treated with androgen antagonist, Cancer Research, 59 (1999) 2511-2515.

[6] M. Korpal, J.M. Korn, X. Gao, D.P. Rakiec, D.A. Ruddy, S. Doshi, J. Yuan, S.G. Kovats, S. Kim, V.G. Cooke, J.E. Monahan, F. Stegmeier, T.M. Roberts, W.R. Sellers, W. Zhou, P. Zhu, An F876L mutation in androgen receptor confers genetic and phenotypic resistance to MDV3100 (enzalutamide), Cancer Discov, 3 (2013) 1030-1043.

[7] T. Yoshida, H. Kinoshita, T. Segawa, E. Nakamura, T. Inoue, Y. Shimizu, T. Kamoto, O. Ogawa, Antiandrogen bicalutamide promotes tumor growth in a novel androgen-dependent prostate cancer xenograft model derived from a bicalutamide-treated patient, Cancer research, 65 (2005) 9611-9616.

[8] H. Wang, Z. Ding, Q.M. Shi, X. Ge, H.X. Wang, M.X. Li, G. Chen, Q. Wang, Q. Ju, J.P. Zhang, M.R. Zhang, L.C. Xu, Anti-androgenic mechanisms of Bisphenol A involve androgen receptor signaling pathway, Toxicology, 387 (2017) 10-16.

[9] J.A. Kemppainen, E. Langley, C.I. Wong, K. Bobseine, W.R. Kelce, E.M. Wilson, Distinguishing androgen receptor agonists and antagonists: distinct mechanisms of activation by medroxyprogesterone acetate and dihydrotestosterone, Molecular endocrinology, 13 (1999) 440-454.

[10] M. Zhang, D. Magit, R. Sager, Expression of maspin in prostate cells is regulated by a positive ets element and a negative hormonal responsive element site recognized by androgen receptor, Proceedings of the National Academy of Sciences of the United States of America, 94 (1997) 5673-5678.

[11] M.A. Fousteris, U. Schubert, D. Roell, J. Roediger, N. Bailis, S.S. Nikolaropoulos, A. Baniahmad, A. Giannis, 20-Aminosteroids as a novel class of selective and complete androgen receptor antagonists and inhibitors of prostate cancer cell growth, Bioorganic & medicinal chemistry, 18 (2010) 6960-6969.

[12] M. Thiele, S. Rabe, W. Hessenkemper, D. Roell, S. Bartsch, F. Kraft, T.E. Abraham, A.B. Houtsmuller, M.E. van Royen, A. Giannis, A. Baniahmad, Novel Nor-Homo- and Spiro-Oxetan-Steroids Target the Human Androgen Receptor and Act as Antiandrogens, Current medicinal chemistry, 22 (2015) 1156-1167.

[13] M. Papaioannou, S. Schleich, I. Prade, S. Degen, D. Roell, U. Schubert, T. Tanner, F. Claessens, R. Matusch, A. Baniahmad, The natural compound atraric acid is an antagonist of the human androgen receptor inhibiting cellular invasiveness and prostate cancer cell growth, Journal of cellular and molecular medicine, 13 (2009) 2210-2223.

[14] R.P.M. Staiger, E.B., Isatoic Anhydride. IV. Reactions with Various Nucleophiles., The Journal of organic chemistry, 24 (1959) 1214-1219.

[15] D. Roell, T.W. Rosler, S. Degen, R. Matusch, A. Baniahmad, Antiandrogenic activity of anthranilic acid ester derivatives as novel lead structures to inhibit prostate cancer cell proliferation, Chemical biology & drug design, 77 (2011) 450-459.

[16] W. Hessenkemper, J. Roediger, S. Bartsch, A.B. Houtsmuller, M.E. van Royen, I. Petersen, M.O. Grimm, A. Baniahmad, A natural androgen receptor antagonist induces cellular senescence in prostate cancer cells, Molecular endocrinology, 28 (2014) 1831-1840.

[17] H. Dotzlaw, M. Papaioannou, U. Moehren, F. Claessens, A. Baniahmad, Agonist-antagonist induced coactivator and corepressor interplay on the human androgen receptor, Mol Cell Endocrinol, 213 (2003) 79-85.

[18] G.P. Dimri, X. Lee, G. Basile, M. Acosta, G. Scott, C. Roskelley, E.E. Medrano, M. Linskens, I. Rubelj, O. Pereira-Smith, et al., A biomarker that identifies senescent human cells in culture and in aging skin in vivo, Proceedings of the National Academy of Sciences of the United States of America, 92 (1995) 9363-9367.

[19] F. Goeman, D. Thormeyer, M. Abad, M. Serrano, O. Schmidt, I. Palmero, A. Baniahmad, Growth inhibition by the tumor suppressor p33ING1 in immortalized and primary cells: involvement of two silencing domains and effect of Ras, Molecular and Cellular Biology, 25 (2005) 422-431.

[20] M.E. van Royen, D.J. van de Wijngaart, S.M. Cunha, J. Trapman, A.B. Houtsmuller, A multi-parameter imaging assay identifies different stages of ligand-induced androgen receptor activation, Cytometry A, 83 (2013) 806-817.

[21] B. He, R.T. Gampe, Jr., A.J. Kole, A.T. Hnat, T.B. Stanley, G. An, E.L. Stewart, R.I. Kalman, J.T. Minges, E.M. Wilson, Structural basis for androgen receptor interdomain and coactivator interactions suggests a transition in nuclear receptor activation function dominance, Molecular Cell, 16 (2004) 425-438.

[22] M.E. van Royen, S.M. Cunha, M.C. Brink, K.A. Mattern, A.L. Nigg, H.J. Dubbink, P.J. Verschure, J. Trapman, A.B. Houtsmuller, Compartmentalization of androgen receptor protein-protein interactions in living cells, The Journal of cell biology, 177 (2007) 63-72.

[23] M.E. van Royen, W.A. van Cappellen, C. de Vos, A.B. Houtsmuller, J. Trapman, Stepwise androgen receptor dimerization, Journal of cell science, 125 (2012) 1970-1979.

[24] P. Farla, R. Hersmus, J. Trapman, A.B. Houtsmuller, Antiandrogens prevent stable DNA-binding of the androgen receptor, Journal of cell science, 118 (2005) 4187-4198.

[25] P. Farla, R. Hersmus, B. Geverts, P.O. Mari, A.L. Nigg, H.J. Dubbink, J. Trapman, A.B. Houtsmuller, The androgen receptor ligand-binding domain stabilizes DNA binding in living cells, Journal of structural biology, 147 (2004) 50-61.

[26] R. Ferraldeschi, C. Pezaro, V. Karavasilis, J. de Bono, Abiraterone and novel antiandrogens: overcoming castration resistance in prostate cancer, Annu Rev Med, 64 (2013) 1-13.